I2R Innovative Imaging & Research

Advanced Noise Reduction Techniques and Improvements

Robert E. Ryan
Mary Pagnutti
Kara Holekamp
Innovative Imaging and Research
Building 1103 Suite 140 C
Stennis Space Center, MS 39529

JACIE/ASPRS 2014
Louisville, KY
March 27, 2014

What is Denoising & Why?

- Denoising is the process of removing noise hopefully without removing information.
  - Edge Preserving Filters
    - Bilateral Filter (Common)
    - Nonlocal Means
    - Sparse Methods (Computationally Intensive)
      - Wavelet
      - SVD
      - DCT Based
      - …

- Improved spatial resolution, increased coverage and acquiring imagery over wider illumination conditions generally decrease SNR

Digital Camera Radiometric Performance

Smaller detectors are needed to keep the sensor size down but decreases SNR if GSD is to be reduced

$$DN = g\,\tau\,A_d\,\frac{\pi}{4\,f\#^2}\int_0^{\infty} L(\lambda)S(\lambda)\,d\lambda$$

$DN - Digital\ Number$
$\lambda - Wavelength$
$L(\lambda) - Spectral\ Radiance$
$S(\lambda) - Spectral\ Response$
$\tau - Integration\ Time$
$g\ - Gain$
$f\# - f - number$

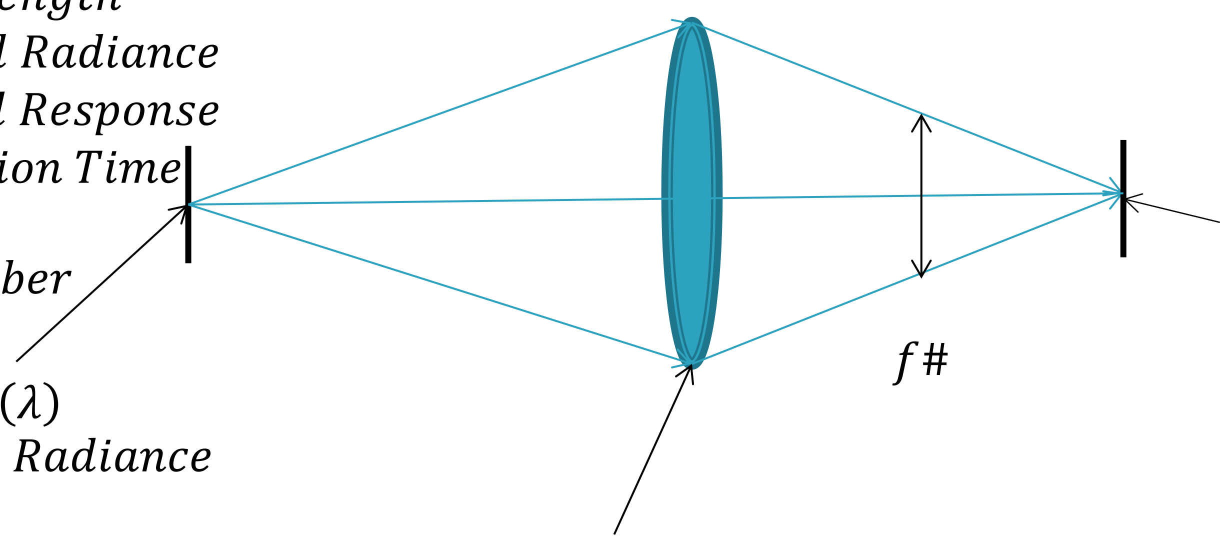

Extending the Imaging Envelope

- Terrestrial optical imaging visible-near infrared (no thermal) in low natural and artificial lighting

- Why?
  - Disaster response for hurricanes, fires, earth quakes, tsunamis, etc. desire all weather all condition imagery
  - Human activity (mapping artificial lights)
  - Light pollution(environmental, astronomy & energy)
  - Improved cloud statistics

Standard
Pan Sharpened
Image

Solar Elev. 0º

Solar Elev. 0º

~ 1-2
Minutes
after sunset

~5 minutes past sunset

Imagery acquired ~10 minutes past sunset

Standard
Pan Sharpened
Imagery

45 minutes
after sunset

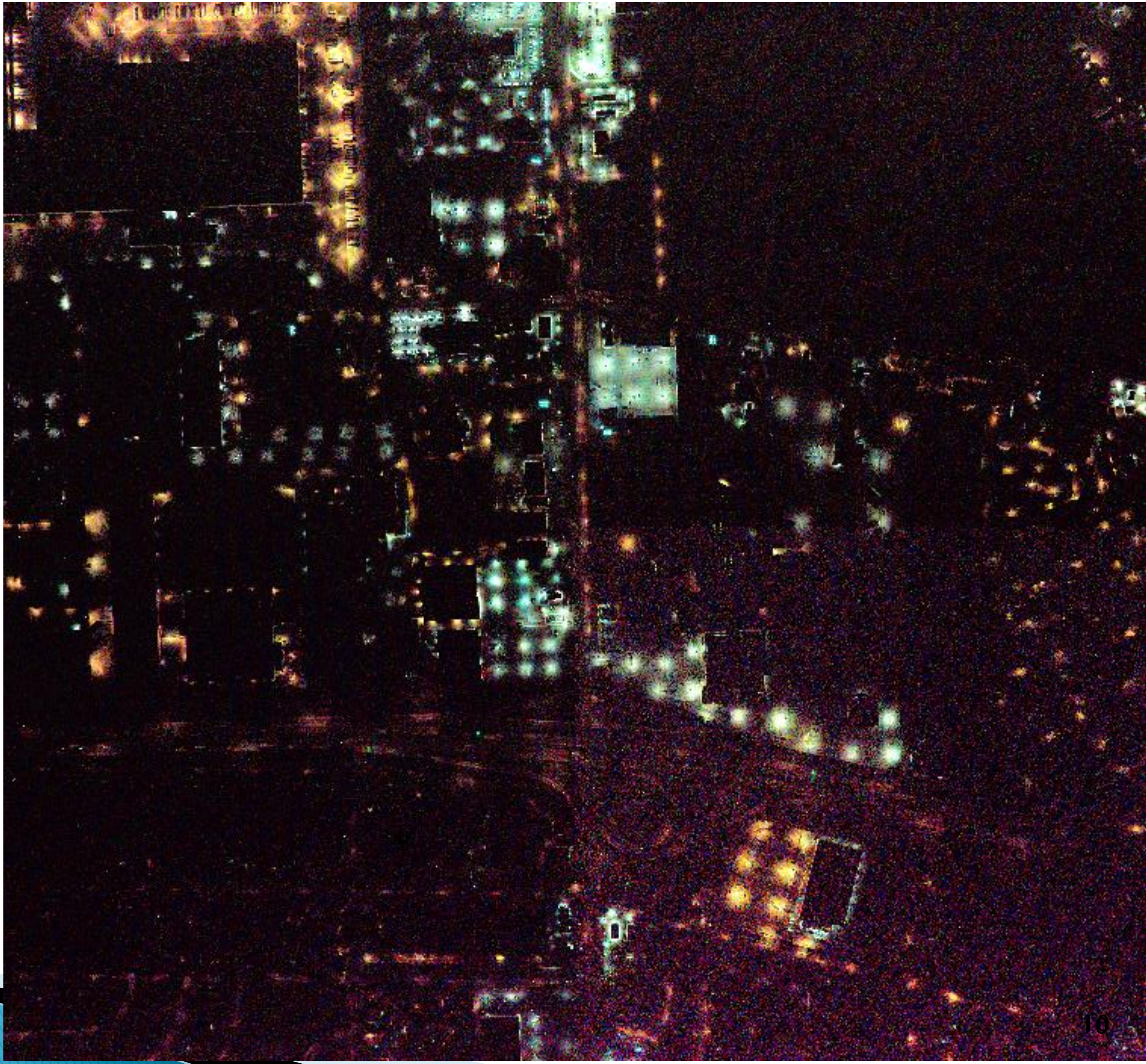

General Denoising Approach

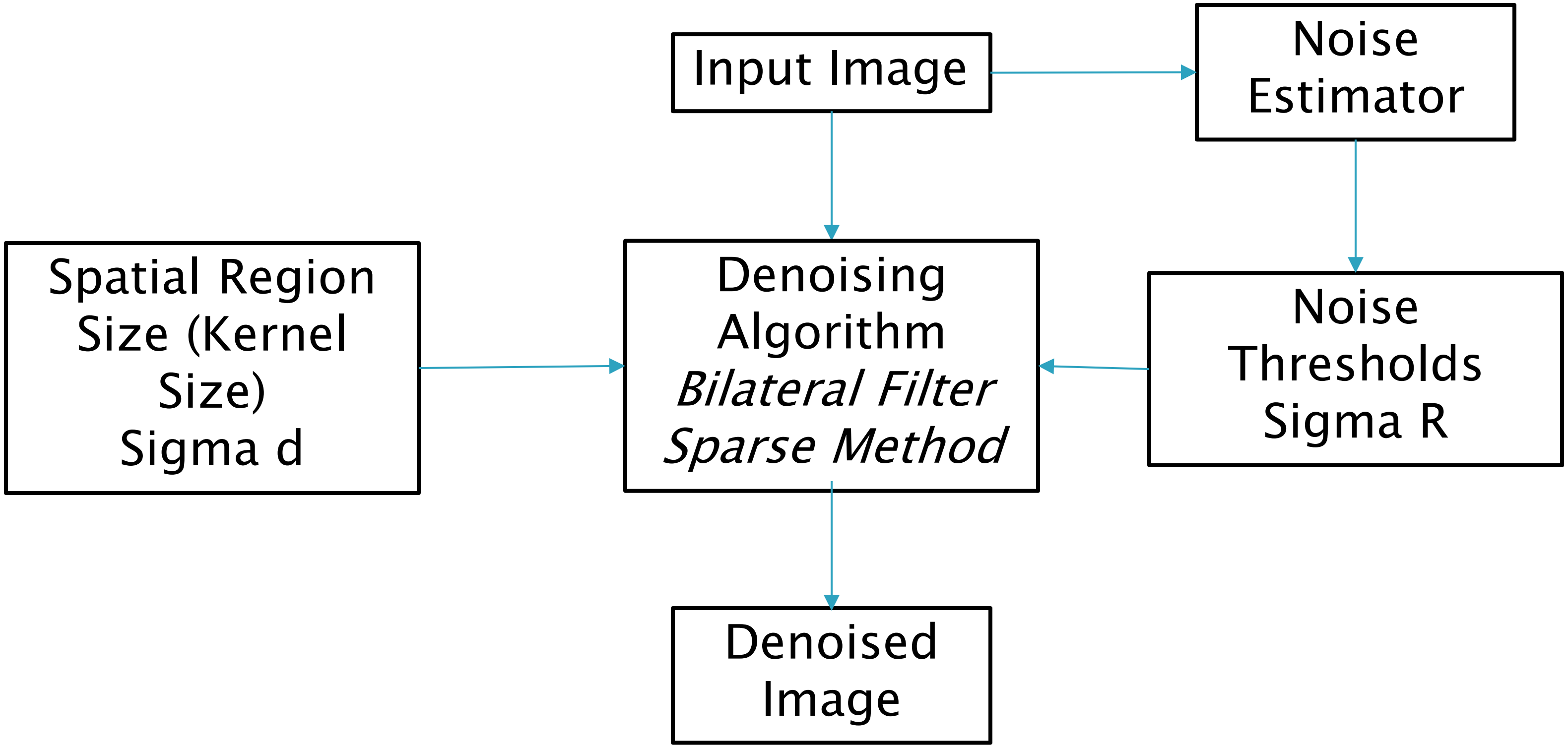

Noise Estimation

- The noise level is needed to set noise thresholds
- Noise depends on both signal levels and sensor characteristics
  - Adaptive noise estimation techniques are needed that work on the imagery of interest

Laboratory Estimation of Noise

- Integrating sphere images can be used estimate variance vs. DN
- Integrating Spheres acquired at different apertures provided imagery at varying DN levels
  - Mean DN and variance values were estimated using a 3x3 moving window
  - Values were grouped into 100DN wide bins and average variance per bin was found
  - Binned DN and variance data from all apertures was combined
- A linear curve fit through the combined binned variance data provided the relationship between DN level and noise

Absolute Radiometric Calibration System

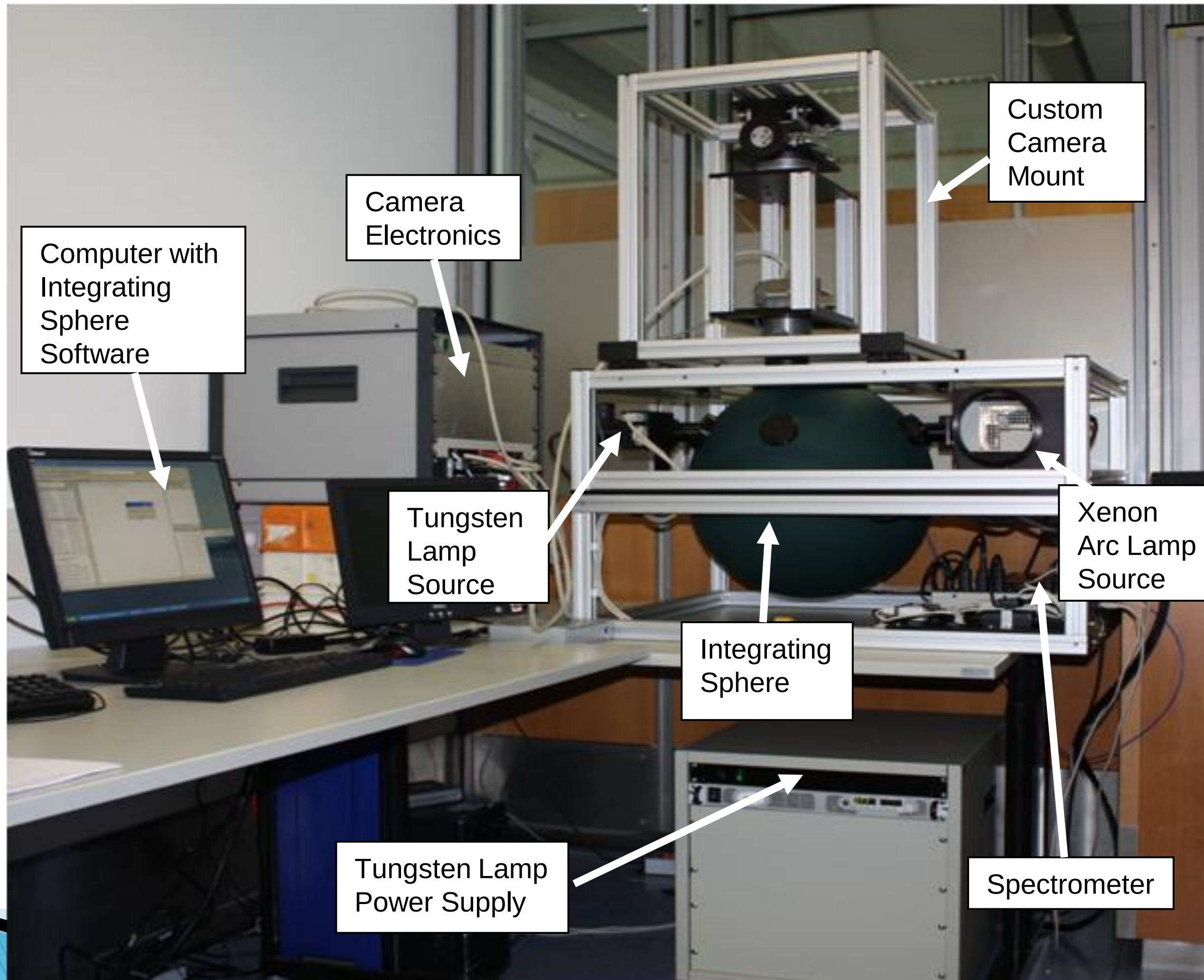

Integrating Sphere Images

- Used to flat field images and measure SNR
- Note SNR will depend on location
- Flat Fielding Image 2D FPA

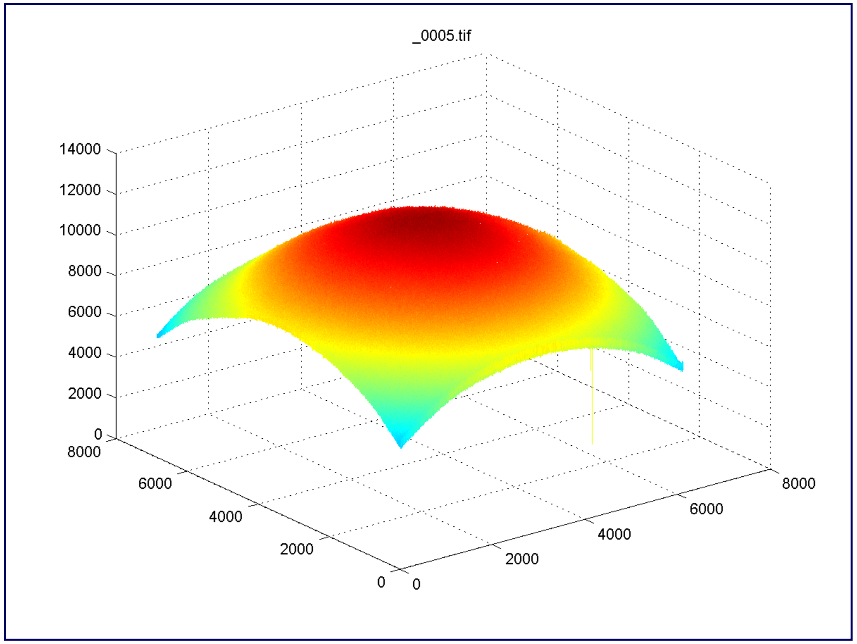

036 Red Band

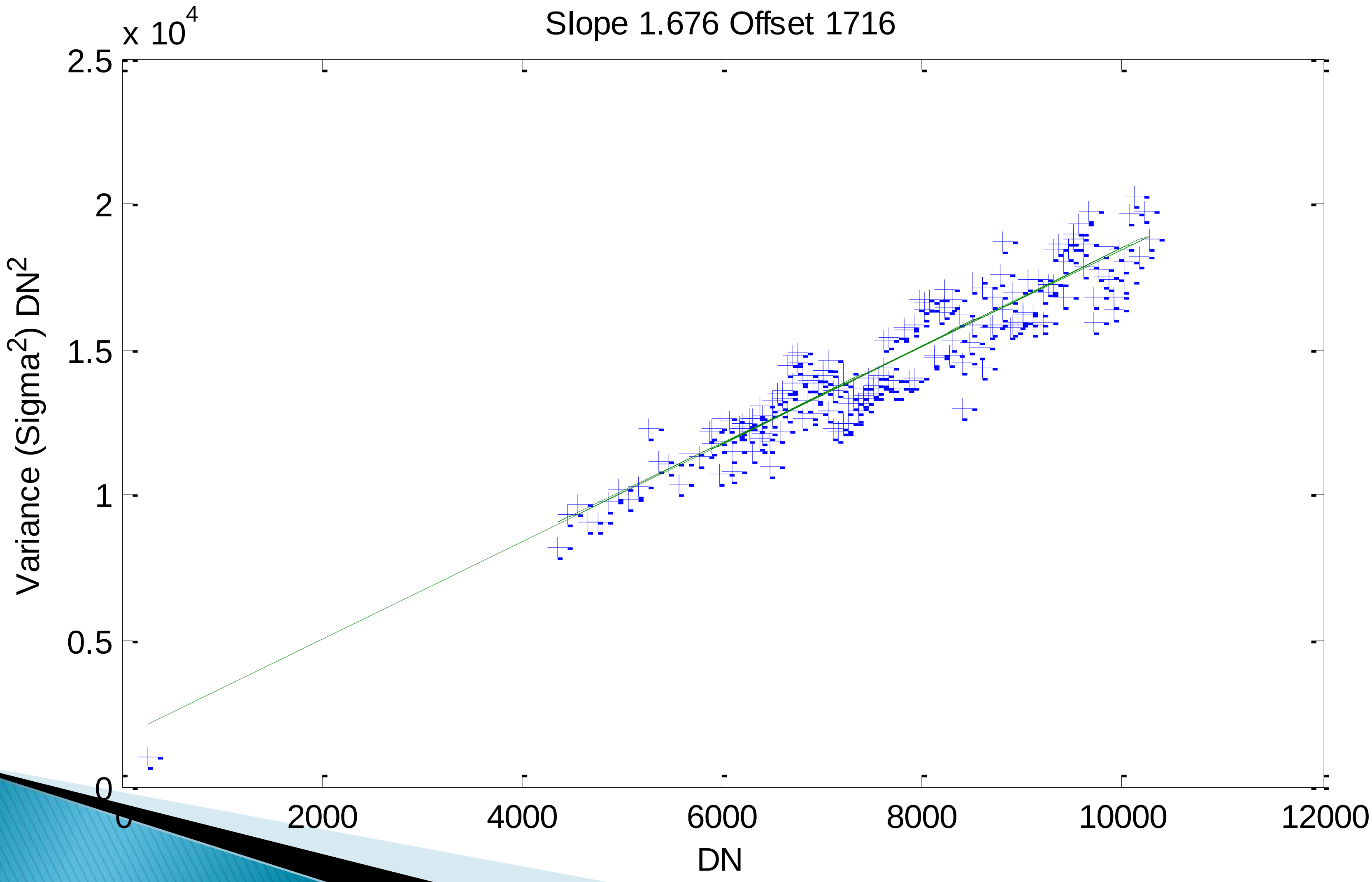

Slope 1.676 Offset 1716
x 10^4
2.5
2
1.5
1
0.5
0
Variance (Sigma^2) DN^2
0
2000
4000
6000
8000
10000
12000
DN

036 Green Band

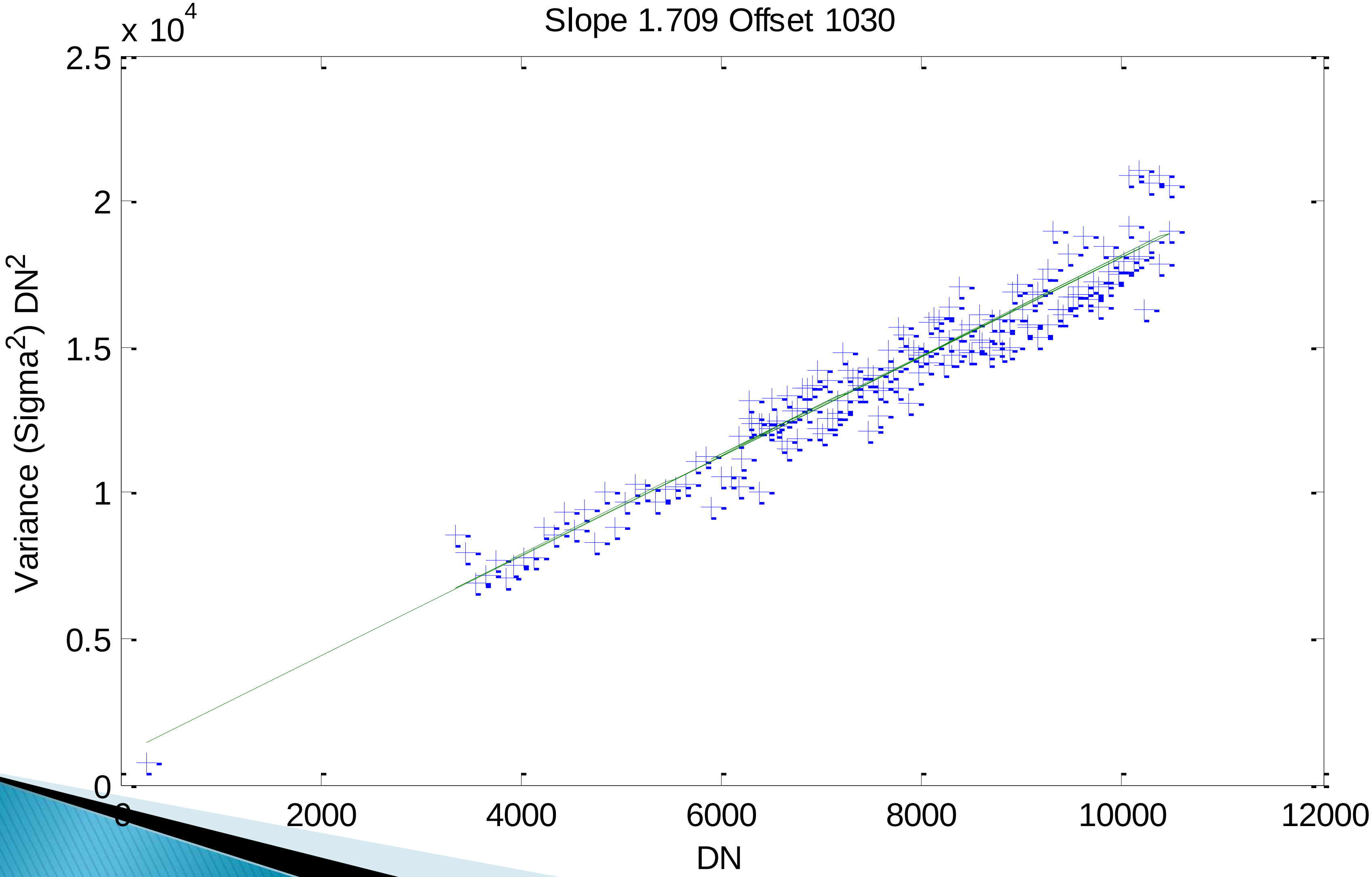

036 Blue Band

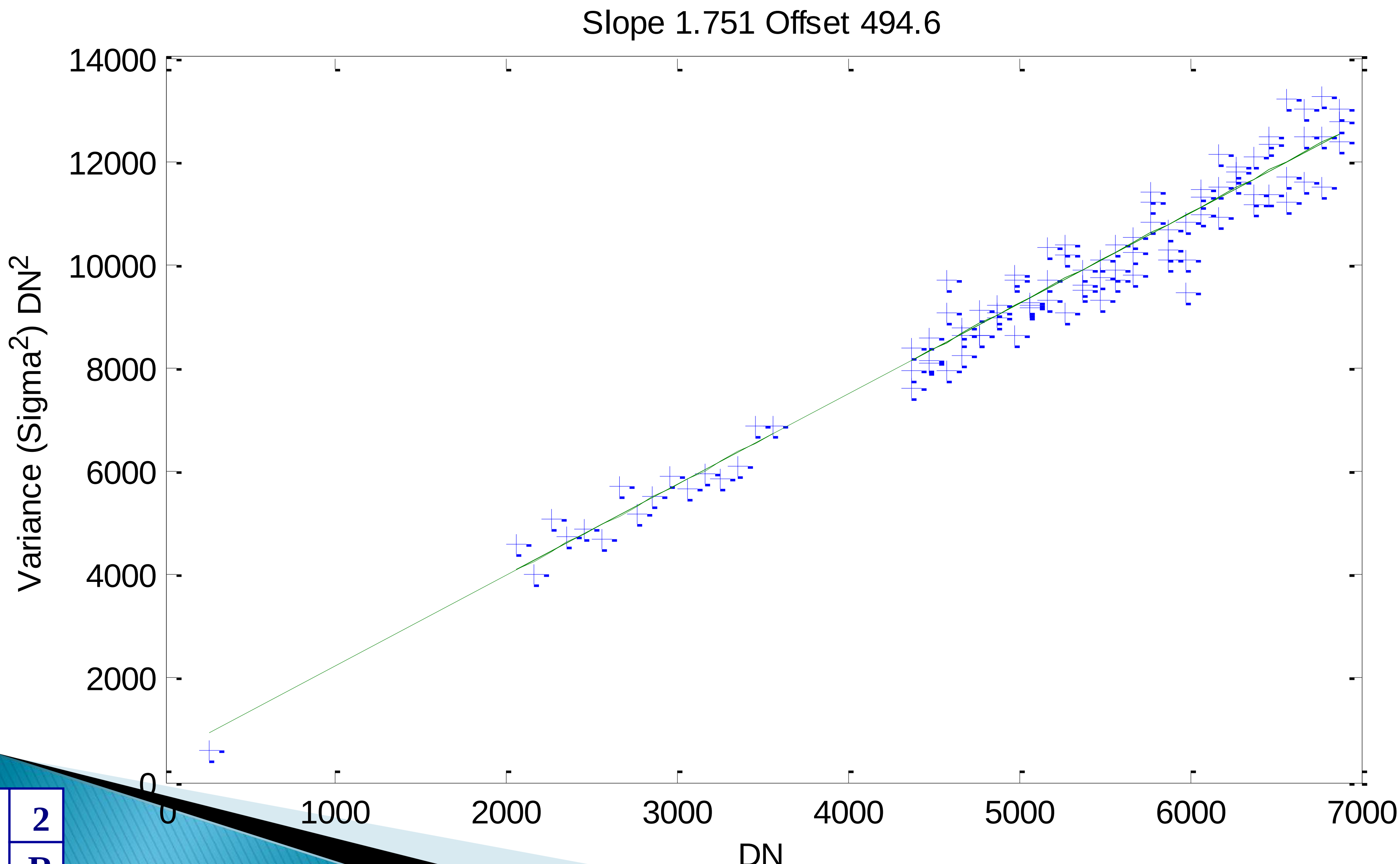

036 NIR Band

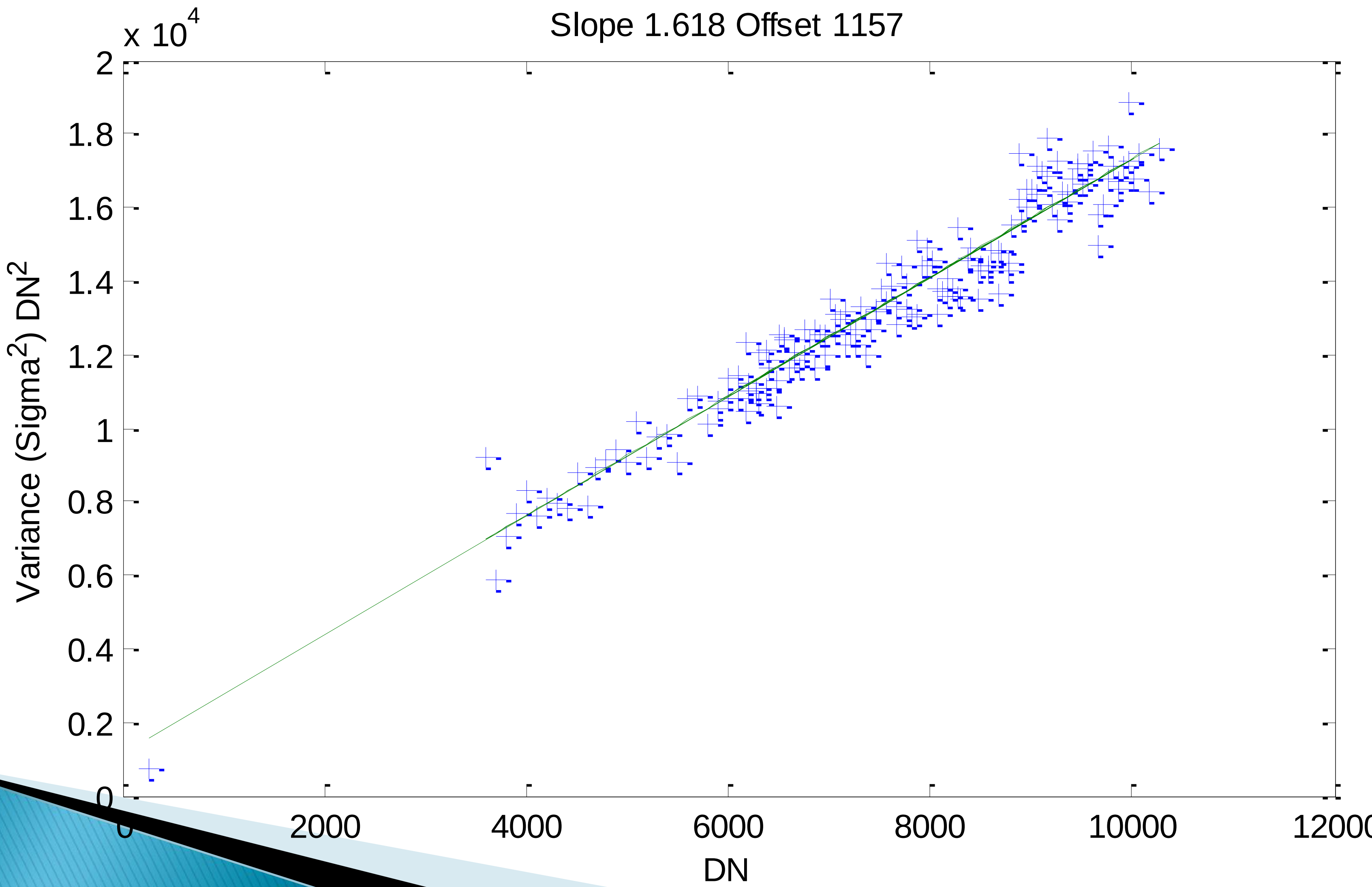
Slope 1.618 Offset 1157
x 10^4
2
1.8
1.6
1.4
1.2
1
0.8
0.6
0.4
0.2
0
Variance (Sigma^2) DN^2
0
2000
4000
6000
8000
10000
12000
DN

Noise Estimation Using Discrete Transforms

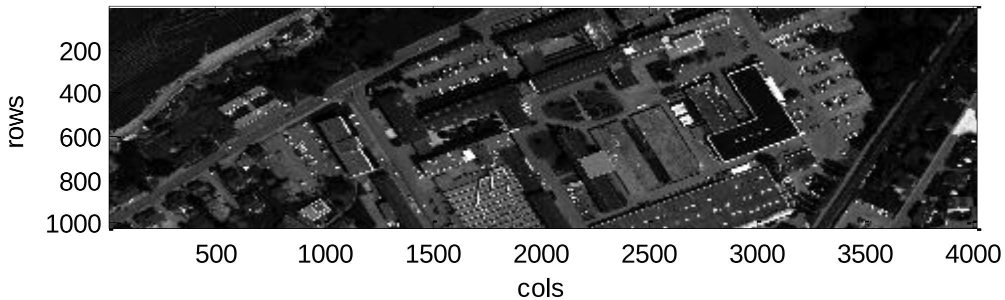

DCT

$$X_{k_1,k_2} = \sum_{n_1=0}^{N_1-1}\left(\sum_{n_2=0}^{N_2-1} x_{n_1,n_2}\cos\left[\frac{\pi}{N_2}\left(n_2+\frac{1}{2}\right)k_2\right]\right)\cos\left[\frac{\pi}{N_1}\left(n_1+\frac{1}{2}\right)k_1\right]$$
$$= \sum_{n_1=0}^{N_1-1}\sum_{n_2=0}^{N_2-1} x_{n_1,n_2}\cos\left[\frac{\pi}{N_1}\left(n_1+\frac{1}{2}\right)k_1\right]\cos\left[\frac{\pi}{N_2}\left(n_2+\frac{1}{2}\right)k_2\right].$$

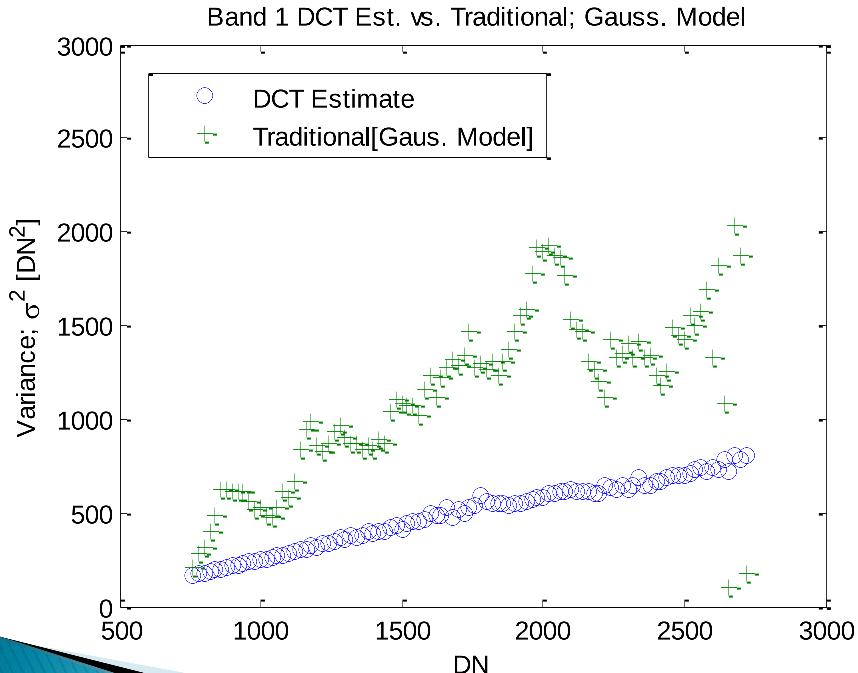

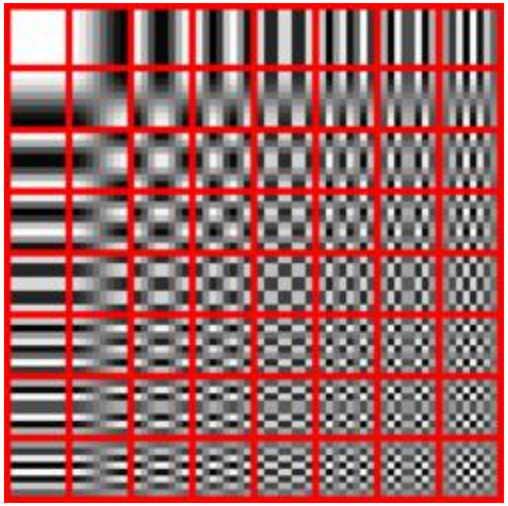

Parseval's Theorem

$$\sum_{n=0}^{N-1}|x[n]|^2 = \frac{1}{N}\sum_{k=0}^{N-1}|X[k]|^2$$

DCT Method Enables Measurement of Noise In Presence of Structure

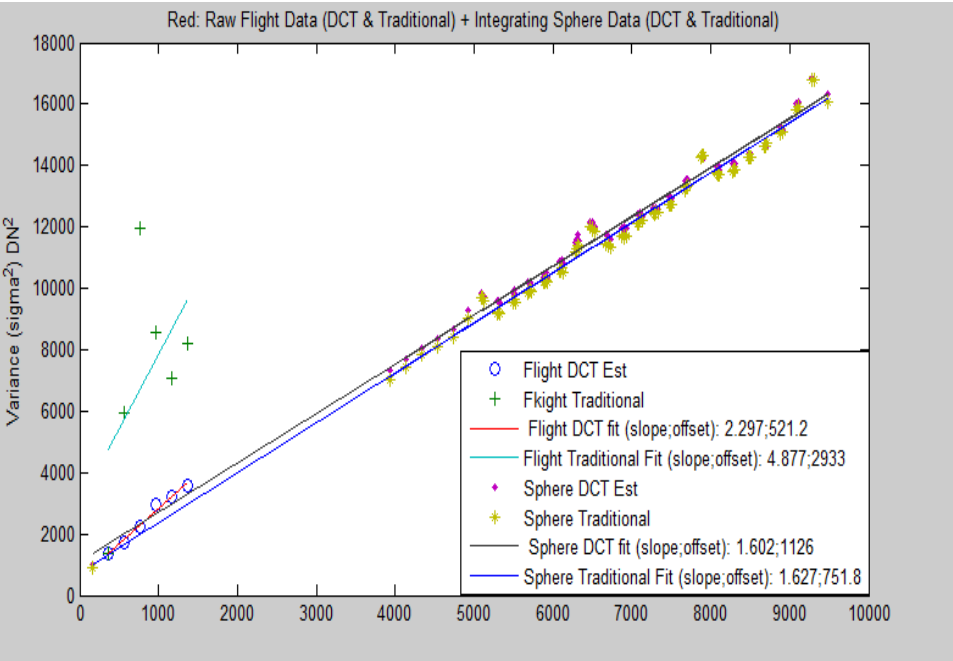
Red: Raw Flight Data (DCT & Traditional) + Integrating Sphere Data (DCT & Traditional)
Variance (sigma^2) DN^2
Flight DCT Est
Fkight Traditional
Flight DCT fit (slope;offset): 2.297;521.2
Flight Traditional Fit (slope;offset): 4.877;2933
Sphere DCT Est
Sphere Traditional
Sphere DCT fit (slope;offset): 1.602;1126
Sphere Traditional Fit (slope;offset): 1.627;751.8

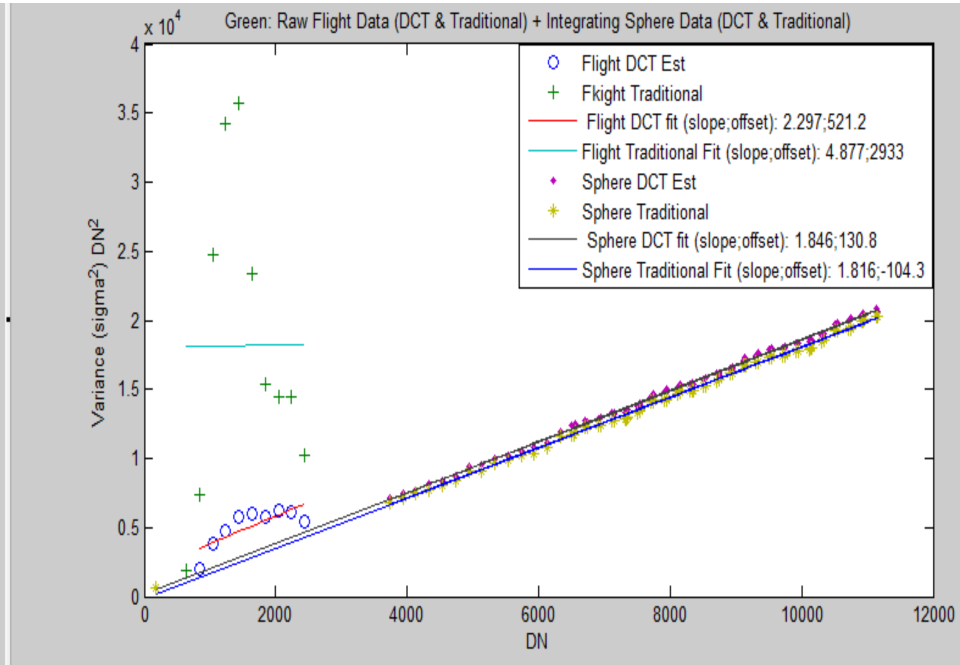
Green: Raw Flight Data (DCT & Traditional) + Integrating Sphere Data (DCT & Traditional)
x 10^4
Variance (sigma^2) DN^2
DN
Flight DCT Est
Fkight Traditional
Flight DCT fit (slope;offset): 2.297;521.2
Flight Traditional Fit (slope;offset): 4.877;2933
Sphere DCT Est
Sphere Traditional
Sphere DCT fit (slope;offset): 1.846;130.8
Sphere Traditional Fit (slope;offset): 1.816;-104.3

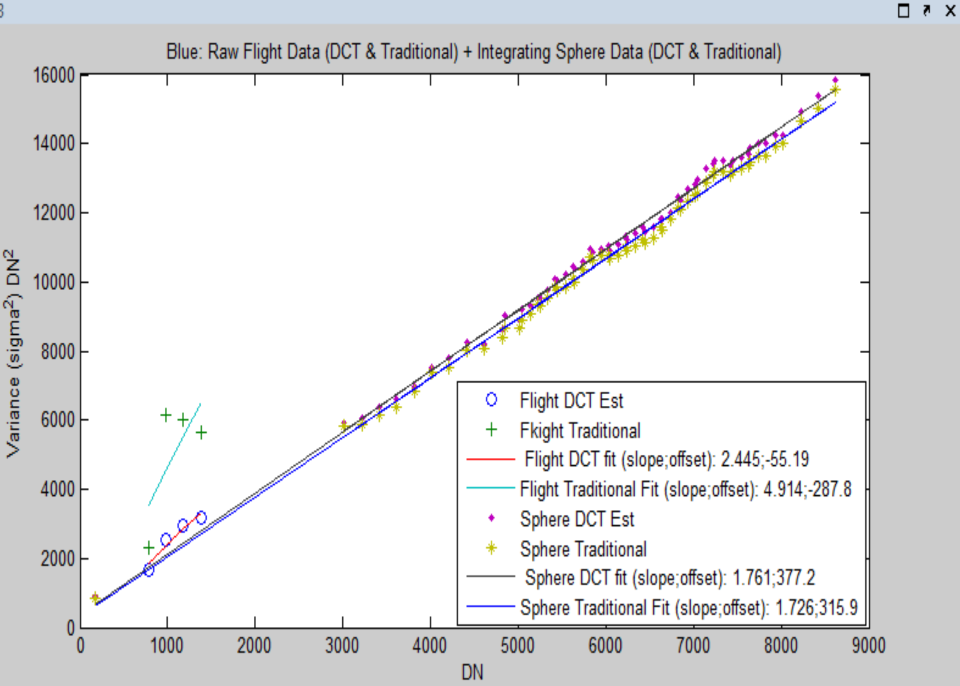
Blue: Raw Flight Data (DCT & Traditional) + Integrating Sphere Data (DCT & Traditional)
Variance (sigma^2) DN^2
DN
Flight DCT Est
Fkight Traditional
Flight DCT fit (slope;offset): 2.445;-55.19
Flight Traditional Fit (slope;offset): 4.914;-287.8
Sphere DCT Est
Sphere Traditional
Sphere DCT fit (slope;offset): 1.761;377.2
Sphere Traditional Fit (slope;offset): 1.726;315.9

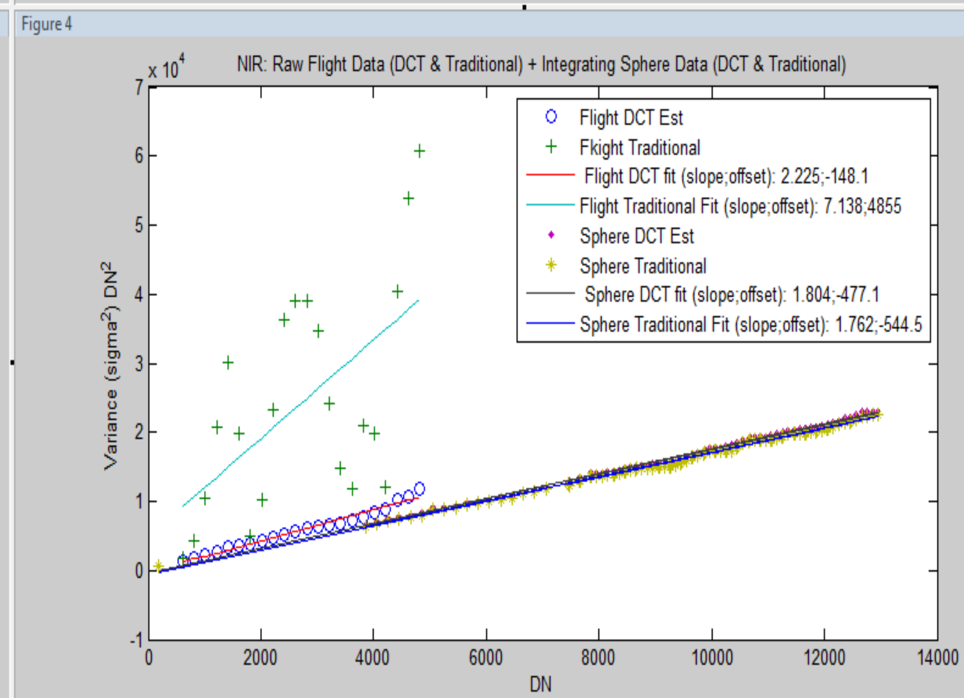
Figure 4
NIR: Raw Flight Data (DCT & Traditional) + Integrating Sphere Data (DCT & Traditional)
x 10^4
Variance (sigma^2) DN^2
DN
Flight DCT Est
Fkight Traditional
Flight DCT fit (slope;offset): 2.225;-148.1
Flight Traditional Fit (slope;offset): 7.138;4855
Sphere DCT Est
Sphere Traditional
Sphere DCT fit (slope;offset): 1.804;-477.1
Sphere Traditional Fit (slope;offset): 1.762;-544.5

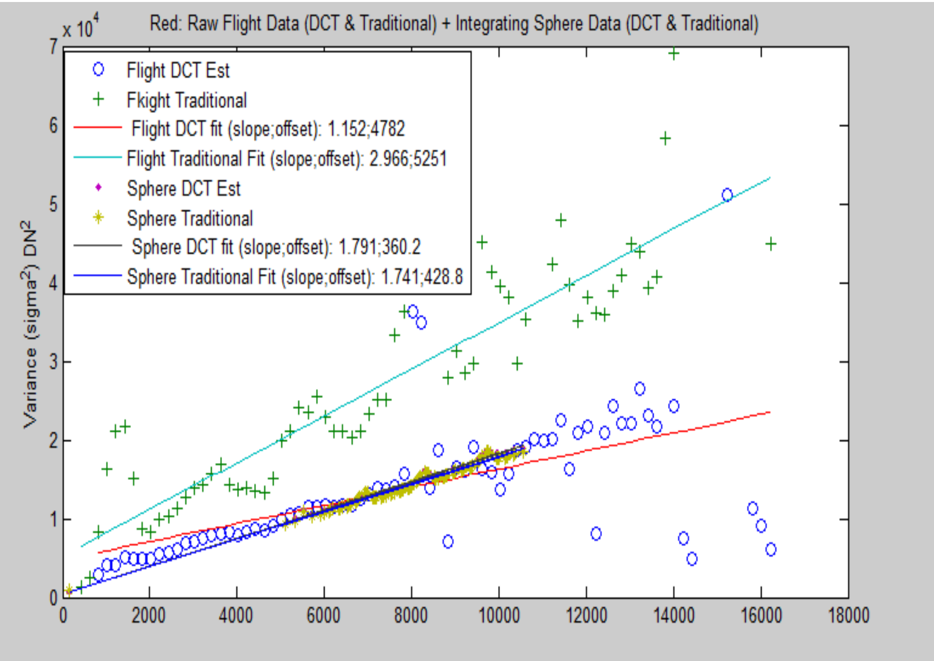
Red: Raw Flight Data (DCT & Traditional) + Integrating Sphere Data (DCT & Traditional)
x 10^4
Variance (sigma^2) DN^2
Flight DCT Est
Fkight Traditional
Flight DCT fit (slope;offset): 1.152;4782
Flight Traditional Fit (slope;offset): 2.966;5251
Sphere DCT Est
Sphere Traditional
Sphere DCT fit (slope;offset): 1.791;360.2
Sphere Traditional Fit (slope;offset): 1.741;428.8

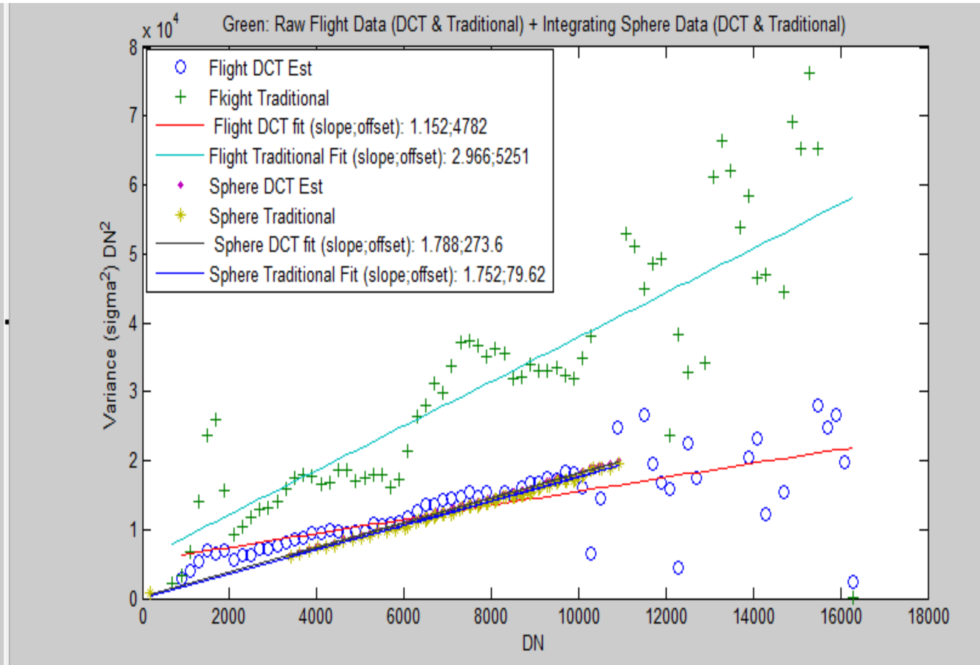
Green: Raw Flight Data (DCT & Traditional) + Integrating Sphere Data (DCT & Traditional)
x 10^4
Variance (sigma^2) DN^2
DN
Flight DCT Est
Fkight Traditional
Flight DCT fit (slope;offset): 1.152;4782
Flight Traditional Fit (slope;offset): 2.966;5251
Sphere DCT Est
Sphere Traditional
Sphere DCT fit (slope;offset): 1.788;273.6
Sphere Traditional Fit (slope;offset): 1.752;79.62

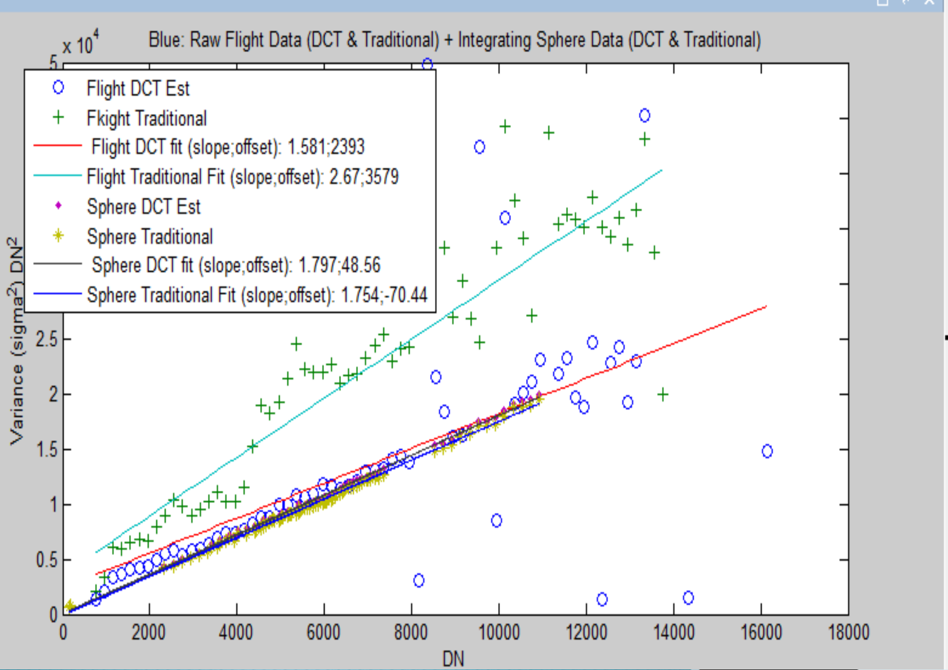
Blue: Raw Flight Data (DCT & Traditional) + Integrating Sphere Data (DCT & Traditional)
x 10^4
Variance (sigma^2) DN^2
DN
Flight DCT Est
Fkight Traditional
Flight DCT fit (slope;offset): 1.581;2393
Flight Traditional Fit (slope;offset): 2.67;3579
Sphere DCT Est
Sphere Traditional
Sphere DCT fit (slope;offset): 1.797;48.56
Sphere Traditional Fit (slope;offset): 1.754;-70.44

Figure 4

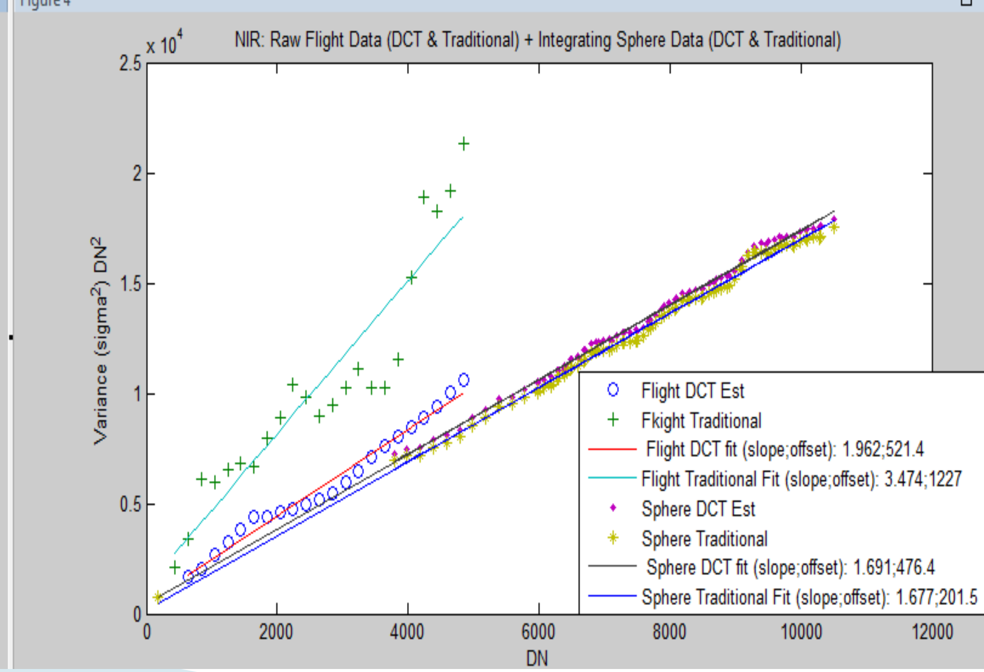
NIR: Raw Flight Data (DCT & Traditional) + Integrating Sphere Data (DCT & Traditional)
x 10^4
Variance (sigma^2) DN^2
DN
Flight DCT Est
Fkight Traditional
Flight DCT fit (slope;offset): 1.962;521.4
Flight Traditional Fit (slope;offset): 3.474;1227
Sphere DCT Est
Sphere Traditional
Sphere DCT fit (slope;offset): 1.691;476.4
Sphere Traditional Fit (slope;offset): 1.677;201.5

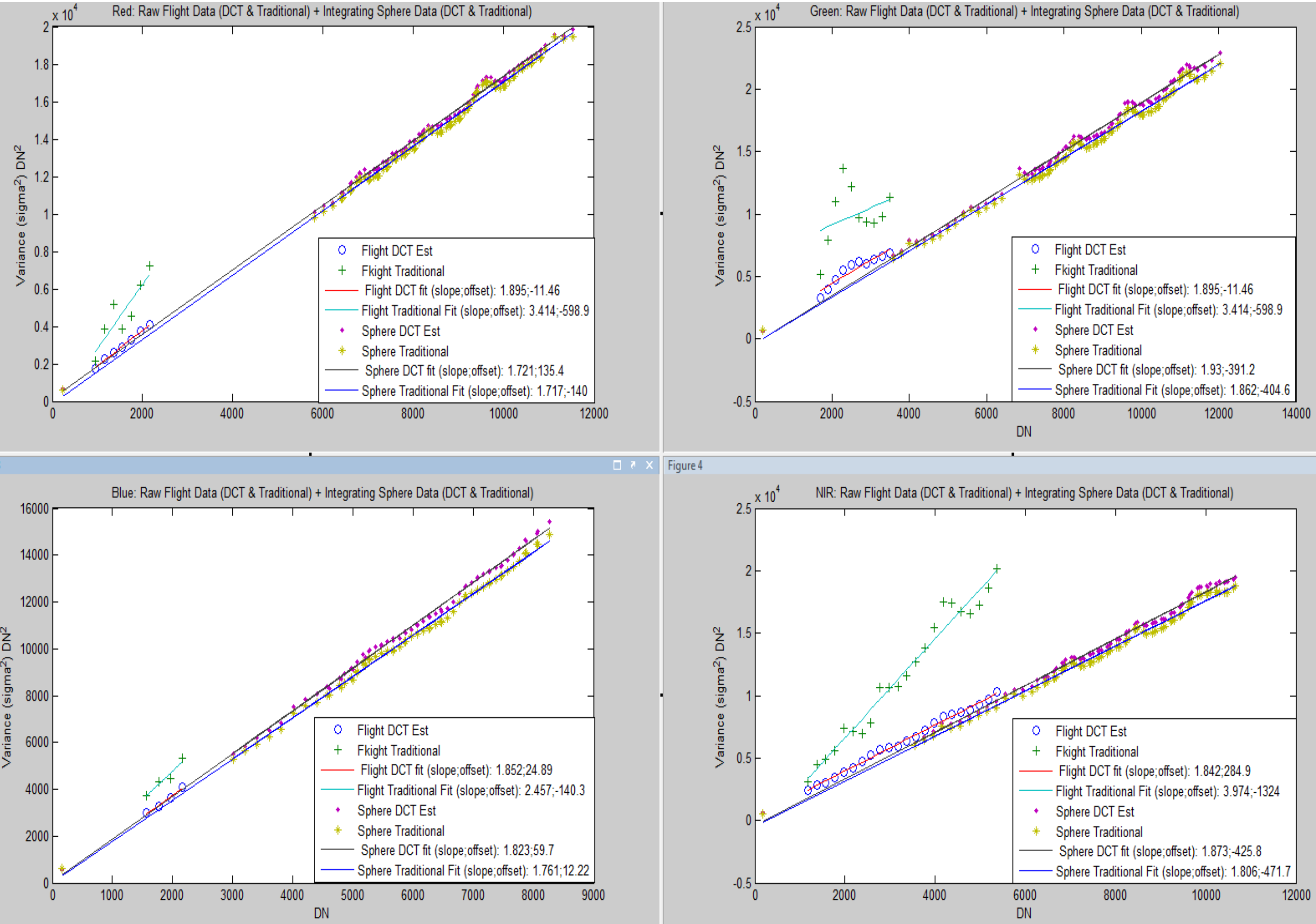
Red: Raw Flight Data (DCT & Traditional) + Integrating Sphere Data (DCT & Traditional)
x 10^4
Variance (sigma^2) DN^2
Flight DCT Est
Fkight Traditional
Flight DCT fit (slope;offset): 1.895;-11.46
Flight Traditional Fit (slope;offset): 3.414;-598.9
Sphere DCT Est
Sphere Traditional
Sphere DCT fit (slope;offset): 1.721;135.4
Sphere Traditional Fit (slope;offset): 1.717;-140
Green: Raw Flight Data (DCT & Traditional) + Integrating Sphere Data (DCT & Traditional)
x 10^4
Variance (sigma^2) DN^2
DN
Flight DCT Est
Fkight Traditional
Flight DCT fit (slope;offset): 1.895;-11.46
Flight Traditional Fit (slope;offset): 3.414;-598.9
Sphere DCT Est
Sphere Traditional
Sphere DCT fit (slope;offset): 1.93;-391.2
Sphere Traditional Fit (slope;offset): 1.862;-404.6
Figure 4
Blue: Raw Flight Data (DCT & Traditional) + Integrating Sphere Data (DCT & Traditional)
Variance (sigma^2) DN^2
DN
Flight DCT Est
Fkight Traditional
Flight DCT fit (slope;offset): 1.852;24.89
Flight Traditional Fit (slope;offset): 2.457;-140.3
Sphere DCT Est
Sphere Traditional
Sphere DCT fit (slope;offset): 1.823;59.7
Sphere Traditional Fit (slope;offset): 1.761;12.22
NIR: Raw Flight Data (DCT & Traditional) + Integrating Sphere Data (DCT & Traditional)
x 10^4
Variance (sigma^2) DN^2
DN
Flight DCT Est
Fkight Traditional
Flight DCT fit (slope;offset): 1.842;284.9
Flight Traditional Fit (slope;offset): 3.974;-1324
Sphere DCT Est
Sphere Traditional
Sphere DCT fit (slope;offset): 1.873;-425.8
Sphere Traditional Fit (slope;offset): 1.806;-471.7

Implementation and Evaluations

- Several selected denoising algorithms were implemented and optimized parameters were determined
  - Exact single band bilateral filter – adaptive noise
  - DCT Patch algorithm
- Algorithms were applied to Aerial images from different acquisitions for testing

Bilateral Filter

- Bilateral filtering is a method of smoothing images that combines two separate types of filtering
  - Spatial filter weights pixels in the neighborhood surround a center pixel based on distance
    - Gaussian function used for spatial filtering
  - Intensity filter weights neighborhood pixels based on the similarity of intensity values
    - Preserves edges by only allowing pixels with similar intensity values to be included in the spatial filter
    - Intensity filter parameter closely related to image noise
- Operates on each band of an image independently

General Bilateral Filter Formulation2

- Spatial Filter
  - $G(p) = \frac{\iint I(q)\ D(q,p)\,dq}{\iint D(q,p)\,dq}$
    - Where I is the input image, p is the neighborhood center pixel, and D is a function of Euclidean distance between pixel q and the center pixel p
- Intensity Filter
  - $F(p) = \frac{\iint I(q)\ R\big(I(q),I(p)\big)\,dq}{\iint R\big(I(q),I(p)\big)\,dq}$
    - Where R is a function of the image intensity between values at neighborhood pixel q and center pixel p
- Combined Bilateral Filter
  - $B(p) = \frac{\iint I(q)\ D(q,p)\ R\big(I(q),I(p)\big)\,dq}{\iint D(q,p)\ R\big(I(q),I(p)\big)\,dq}$

Implemented Gaussian Bilateral Filter2

- Gaussian Spatial Function
  - $D(q,p) = e^{-\left(\frac{(x-c)^2+(y-r)^2}{2\sigma_D{}^2}\right)}$
    - Where, (x,y) and (r,c) are the image row/column locations of pixels q and p, and the standard deviation, σD, defines the width of the gaussian function
- Gaussian Intensity Function
  - $R(I(q),I(p)) = e^{-\left(\frac{(I(q)-I(p))^2}{2\sigma_R{}^2}\right)}$
    - Where, I(q) and I(p) are the image intensity values at pixels q and p, and the standard deviation, σR, defines the width of the intensity range
- Bilateral Filter
  - $B(p) = \frac{\sum_q I(q)\ D(q,p)\ R(I(q),I(p))}{\sum_q D(q,p)\ R(I(q),I(p))}$

Bilateral Filter Test Parameters

- Test edge
  - 51 x 51 pixels (= neighborhood size)
  - Maximum image intensity (DN) = 1000
- Image noise varied between 2 and 4 % of maximum DN
- σ_D varied between 5 and 10
- σ_R varied between 1, 2, and 5 times the image noise

Test Edge – $\sigma_D = 5$ Image Noise = 2% of Max

Input Image

PSNR= 34.5

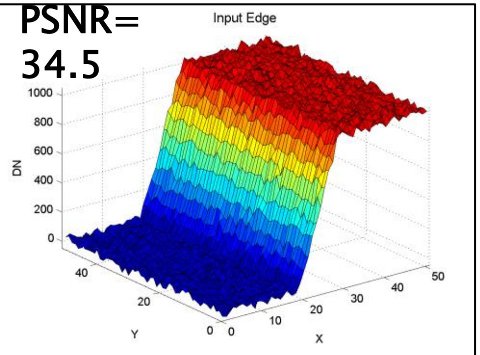

Spatial Filter

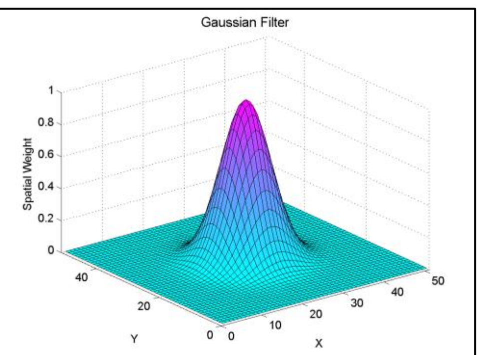

Intensity Filter

σ_R = Noise

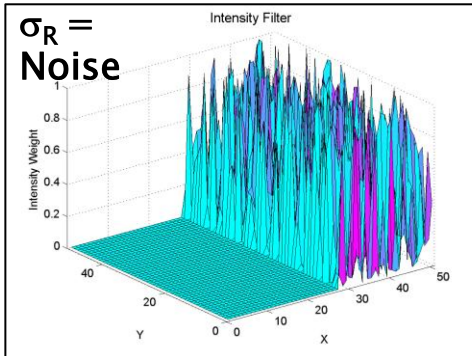

σ_R = 2*Noise

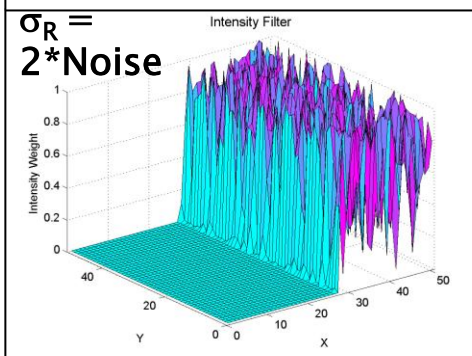

σ_R = 5*Noise

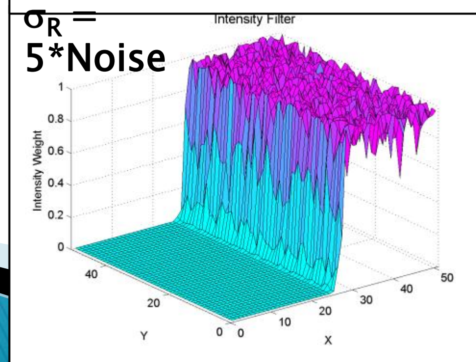

Bilateral Filter

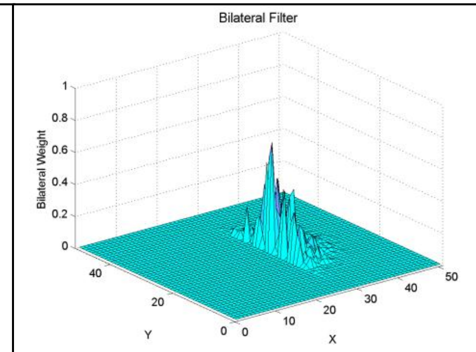

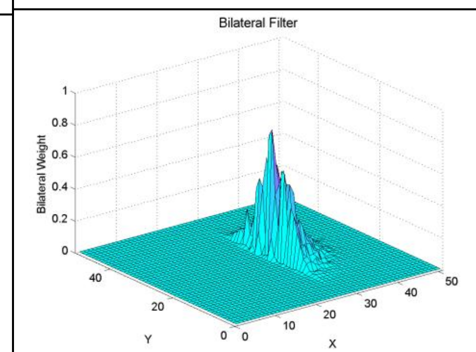

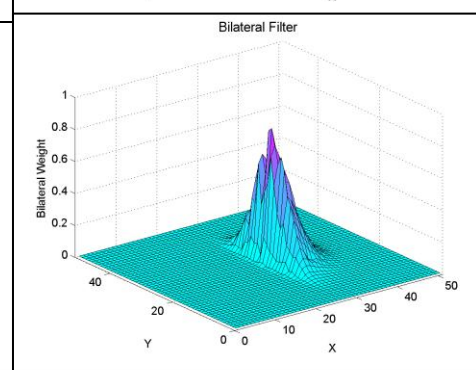

Output Image

PSNR= 42.7

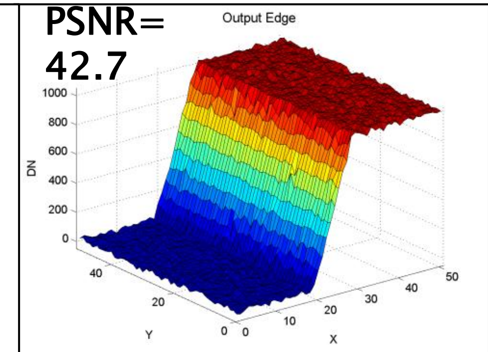

PSNR= 38.1

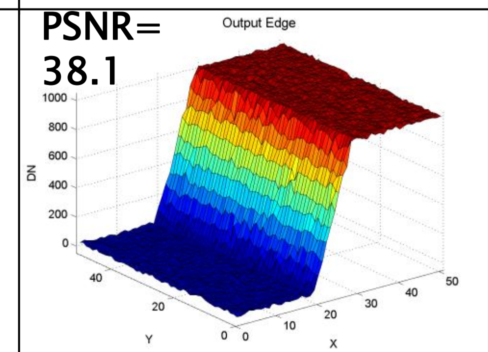

PSNR= 30.6

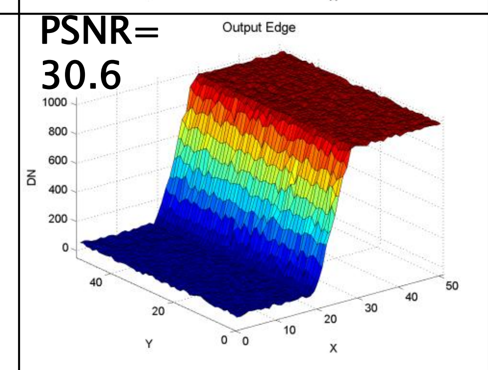

Test Edge – σ_D = 10
Image Noise = 2% of Max DN

Input Image

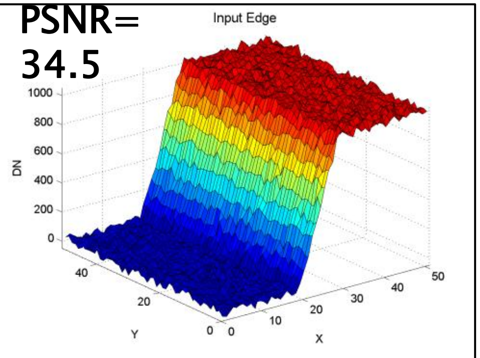

Spatial Filter

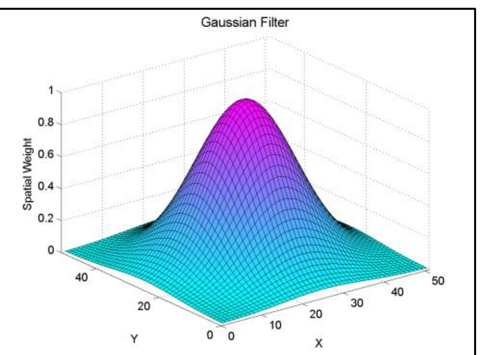

Intensity Filter | Bilateral Filter | Output Image

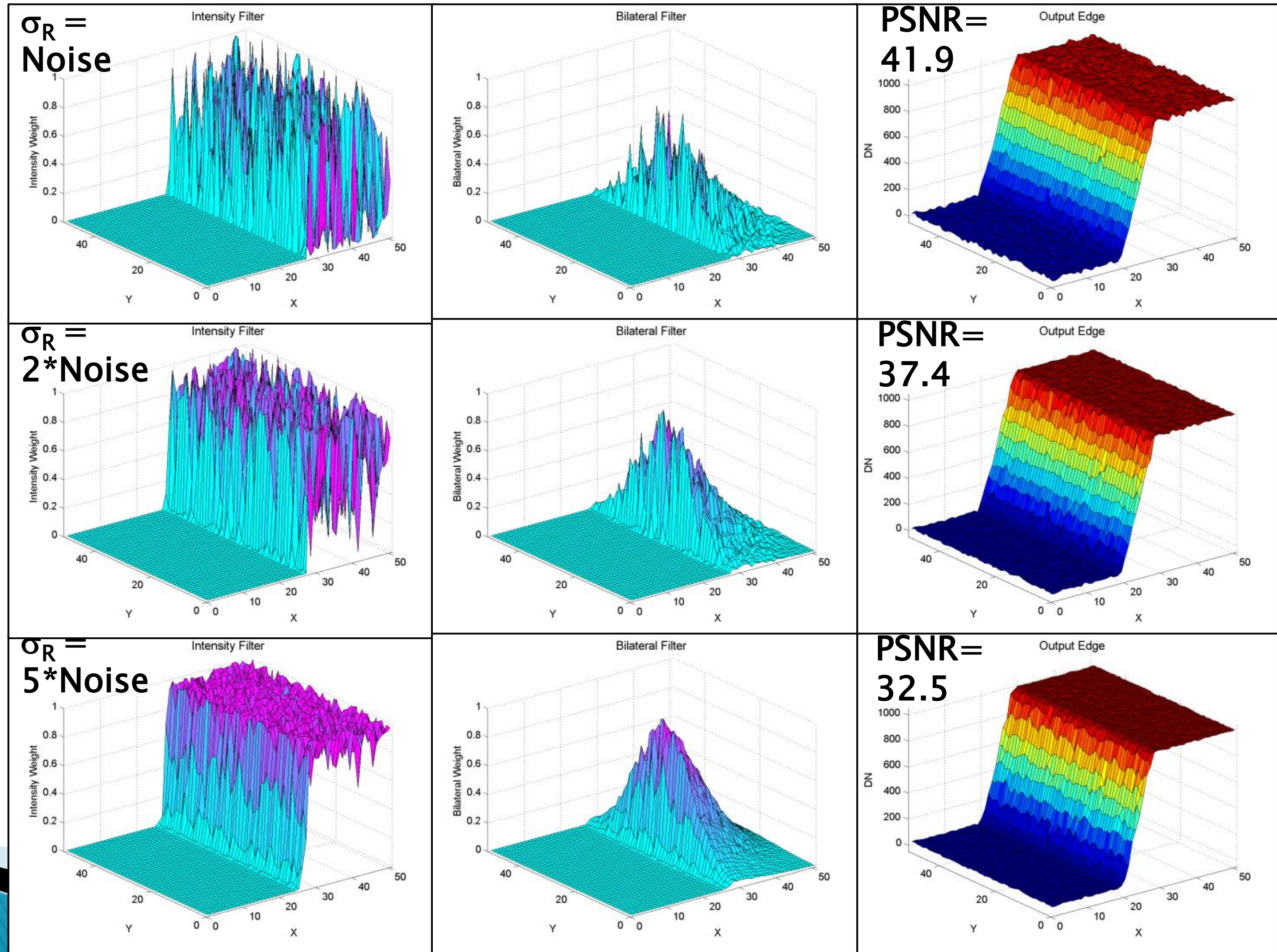

Test Edge – $\sigma_D = 5$
Image Noise = 4% of Max DN

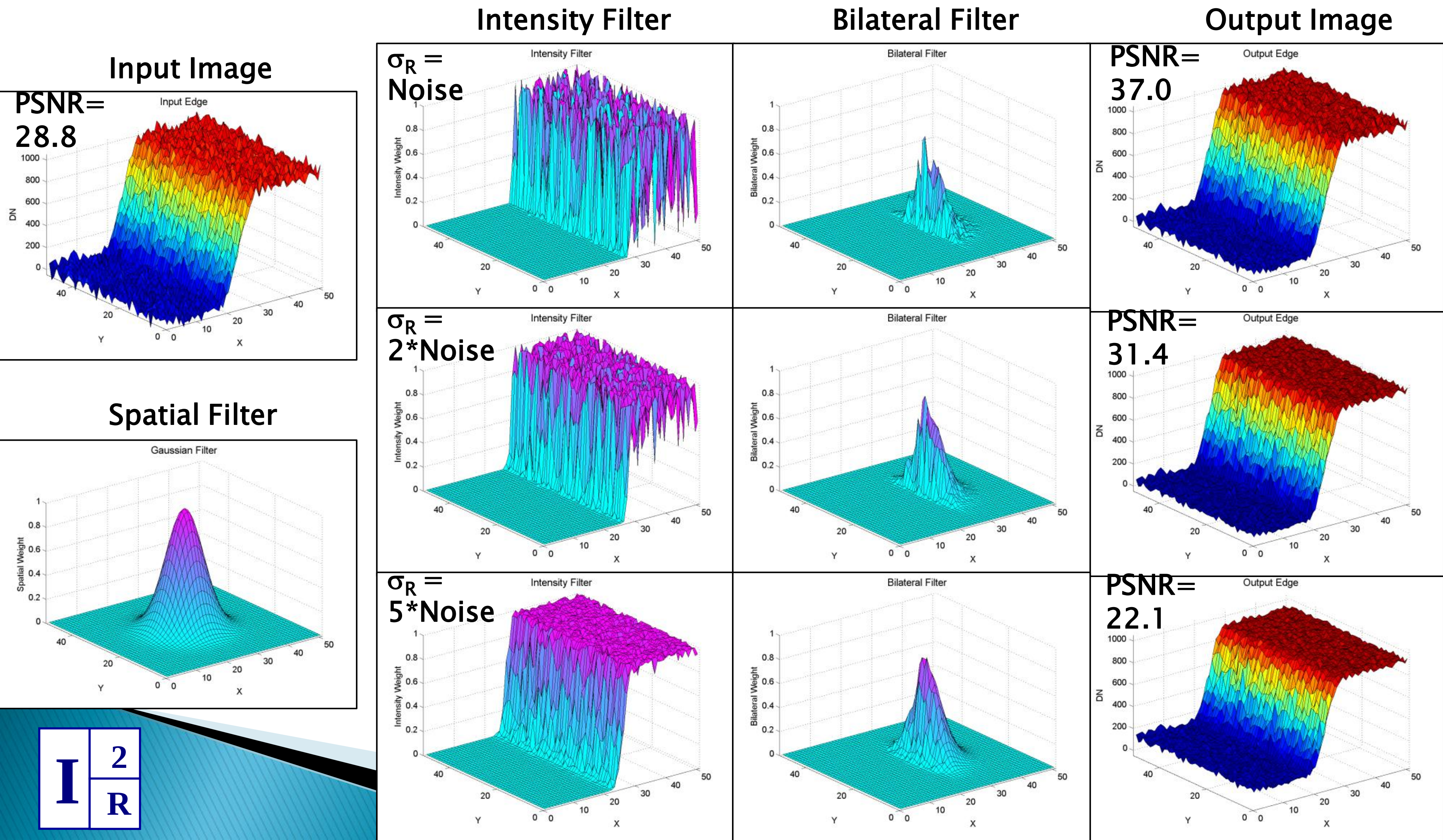

Test Edge – $\sigma_D = 10$ Image Noise = 4% of Max DN

Input Image

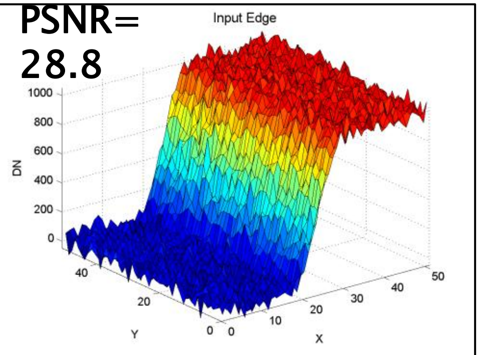

Spatial Filter

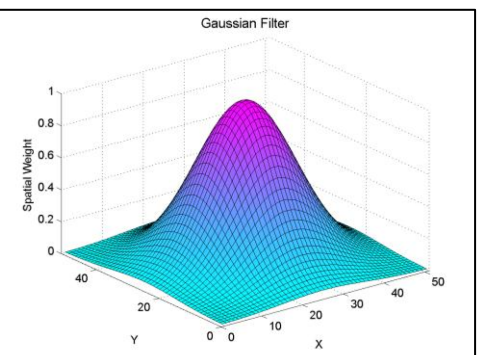

Intensity Filter | Bilateral Filter | Output Image

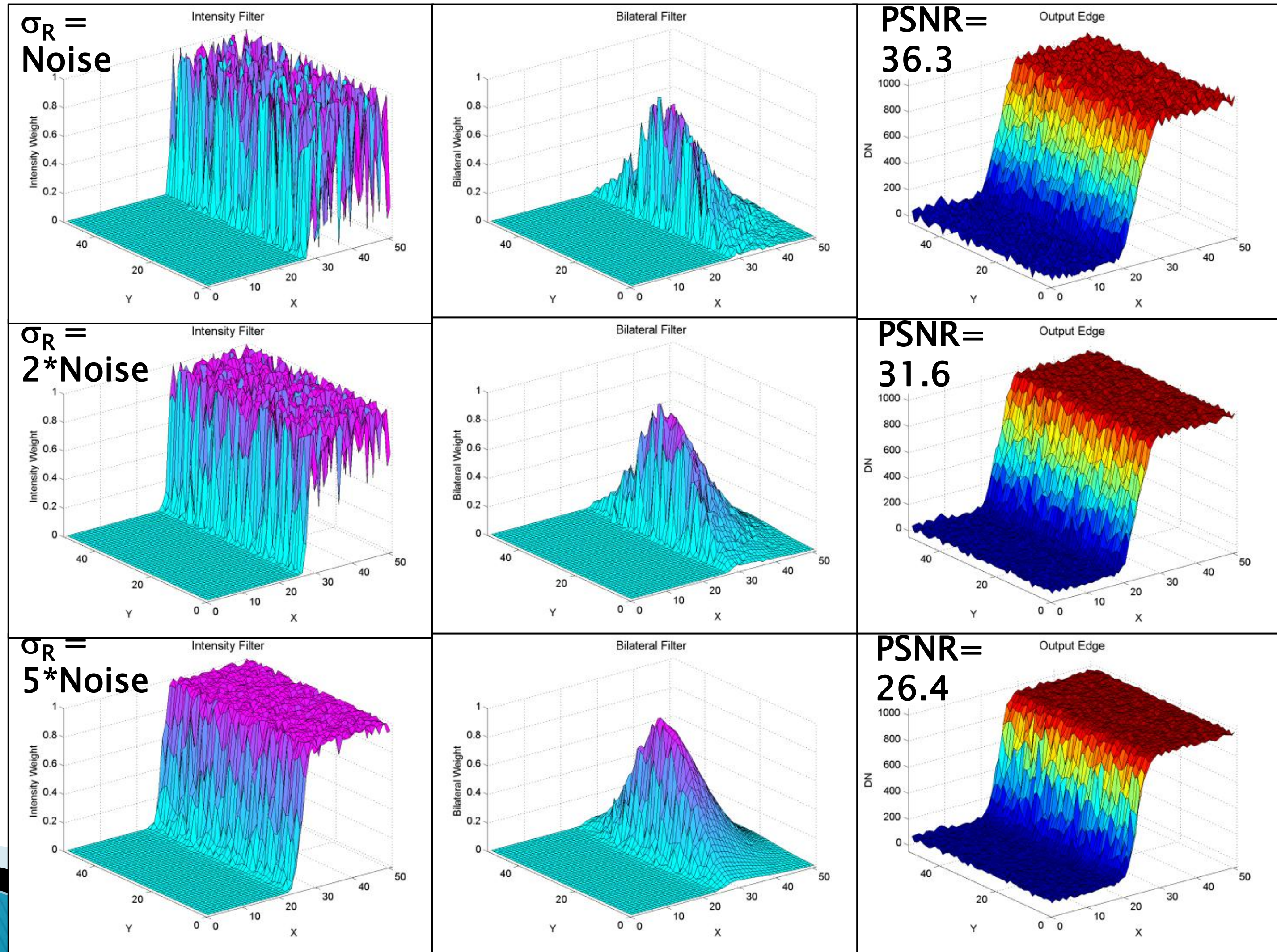

Example Image Results

- Sample areas taken from Stennis and Wbroad images

Exact Bilateral Filter with Adaptive Noise

Unfiltered

Filtered

W_broad_2010_001~086_msrgbn.tif

DCT Patch with Adaptive Noise

Unfiltered

Filtered

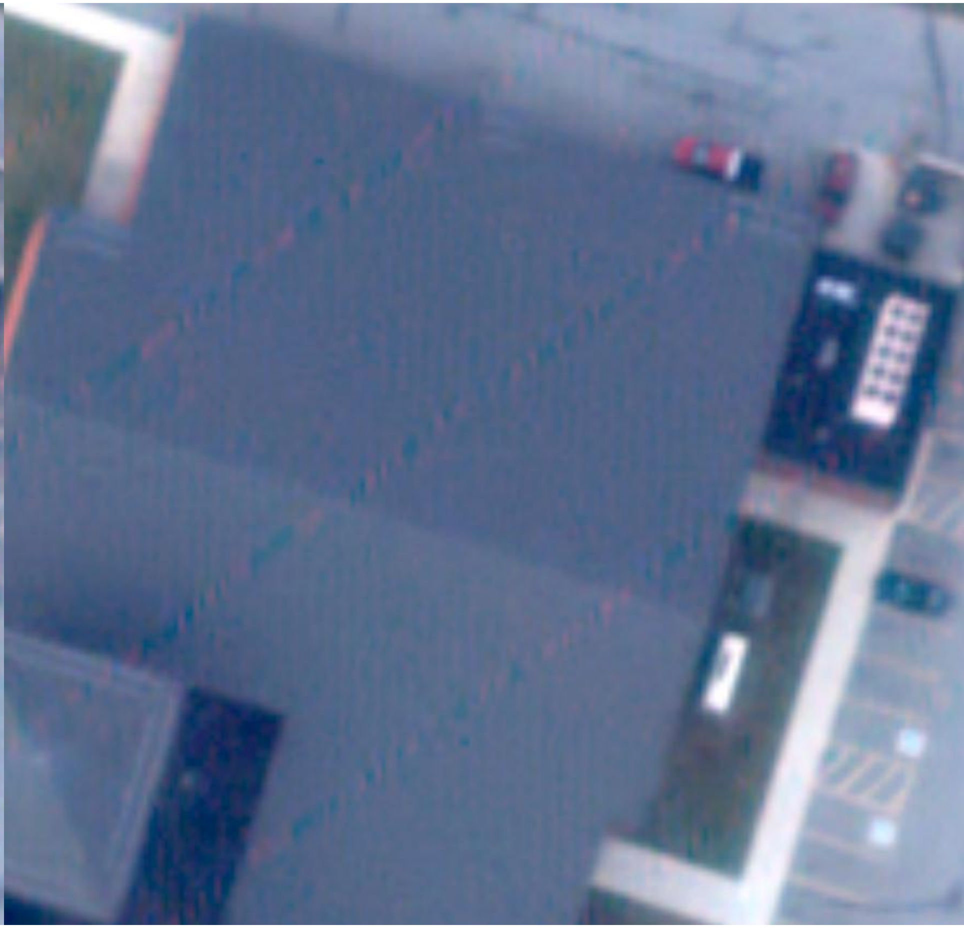

W_broad_2010_001~086_msrgbn.tif

Exact Bilateral Filter with Adaptive Noise

Unfiltered

Filtered

W_broad_2010_001~086_msrgbn.tif

DCT Patch with Adaptive Noise

Unfiltered

Filtered

W_broad_2010_001~086_msrgbn.tif

Exact Bilateral Filter with Adaptive Noise

Unfiltered

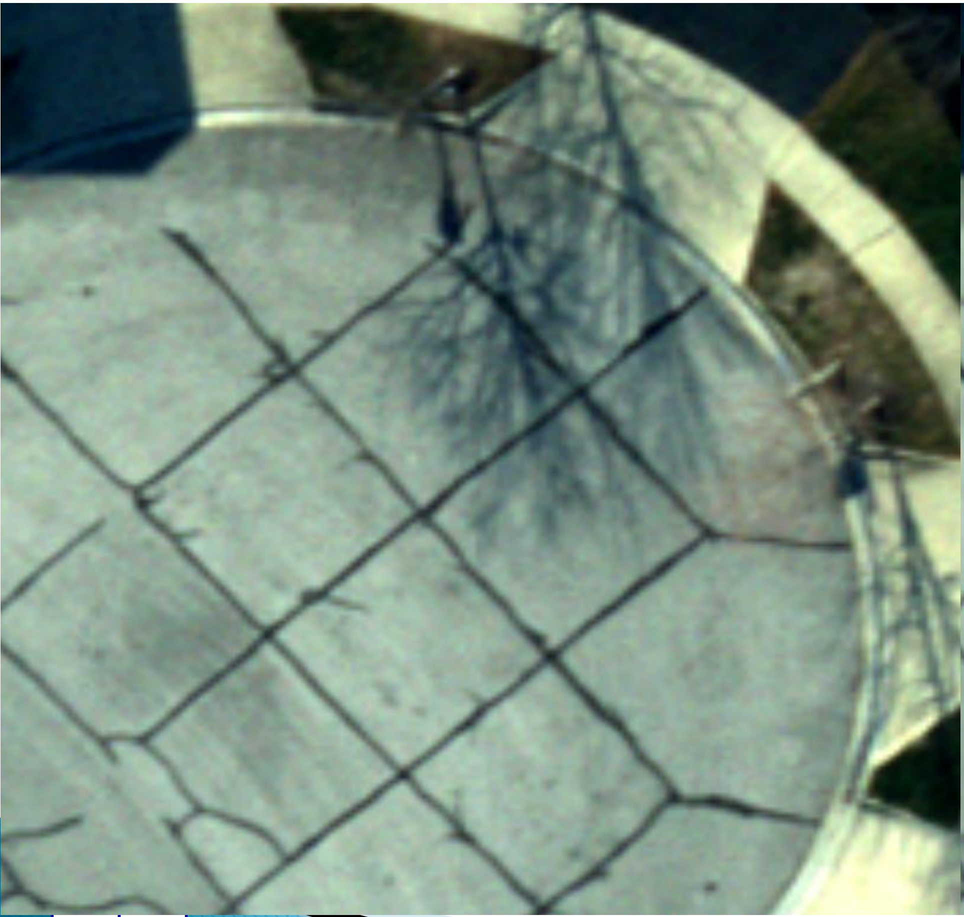

Filtered

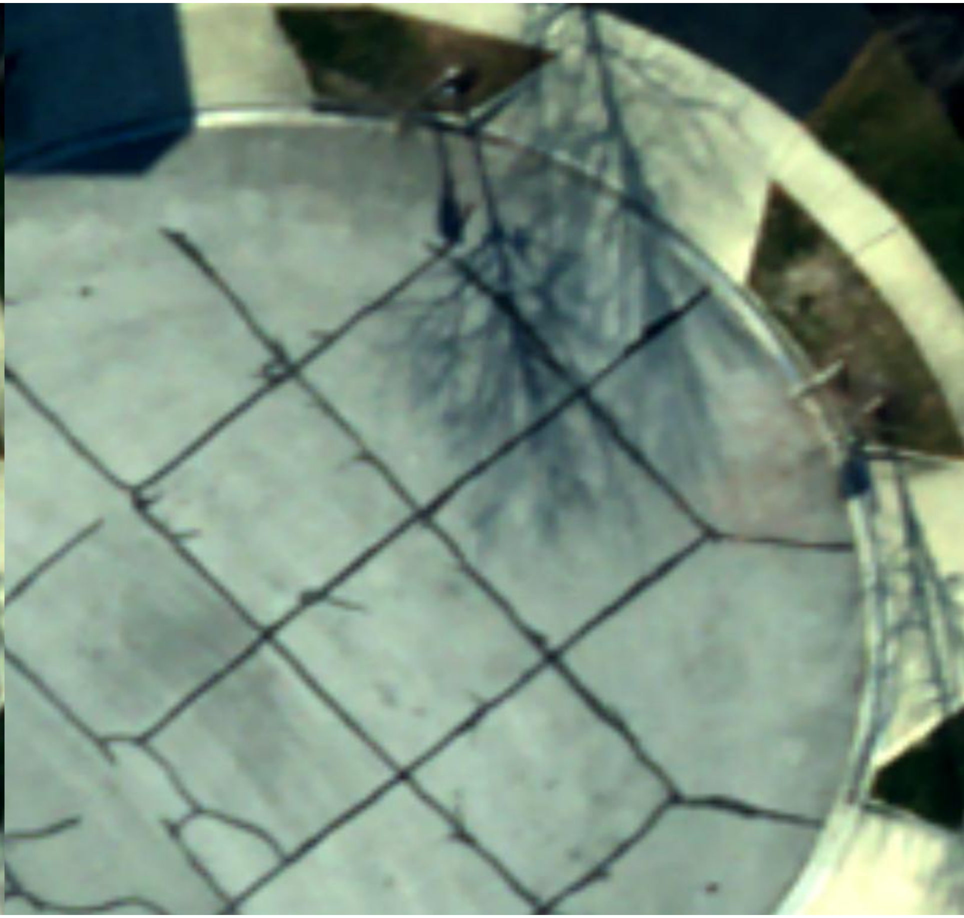

Geobore_5cm_003~0001_msrgbn.tif

DCT Patch with Adaptive Noise

Unfiltered Filtered

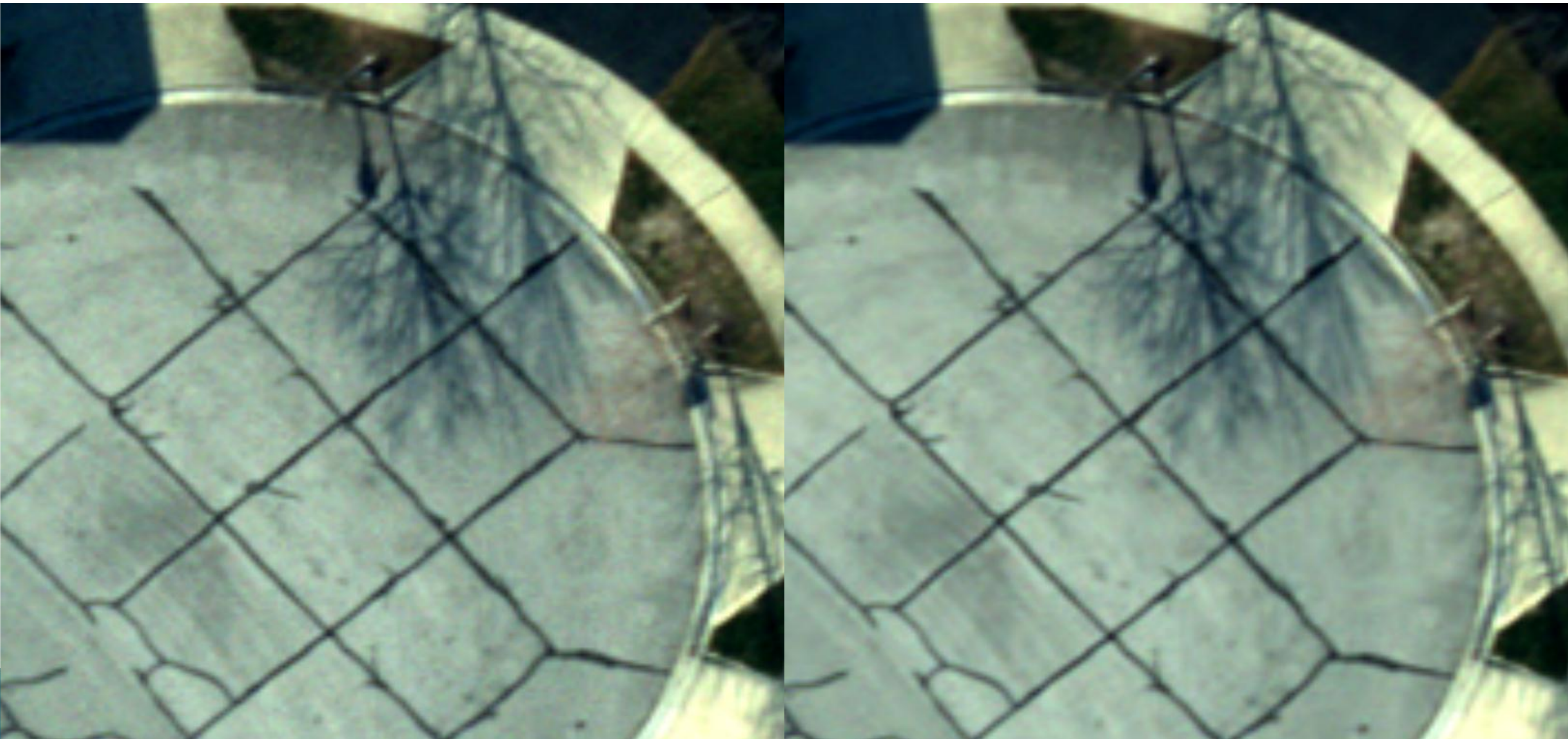

Geobore_5cm_003~0001_msrgbn.tif

Exact Bilateral Filter with Adaptive Noise

Gavle_20cm_01~0057_msrgbn.tif

DCT Patch with Adaptive Noise

Unfiltered

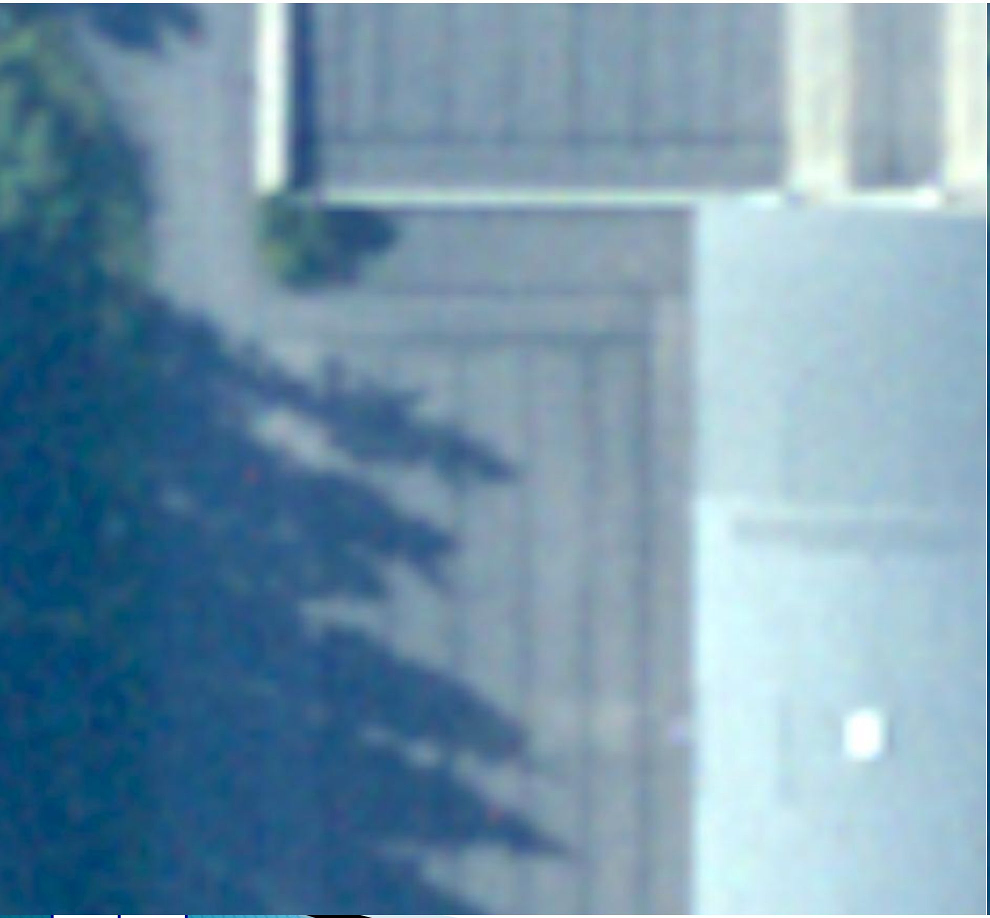

Filtered

Gavle_20cm_01~0057_msrgbn.tif

Exact Bilateral Filter with Adaptive Noise

Unfiltered

Filtered

Gavle_20cm_01~0057_msrgbn.tif

DCT Patch with Adaptive Noise

Unfiltered

Filtered

DCT Pan Filtering Examples

DMCII Low Light data acquired over Columbus OH

GSD: 36 cm (MS) and 17.6cm (pan)

Example 1

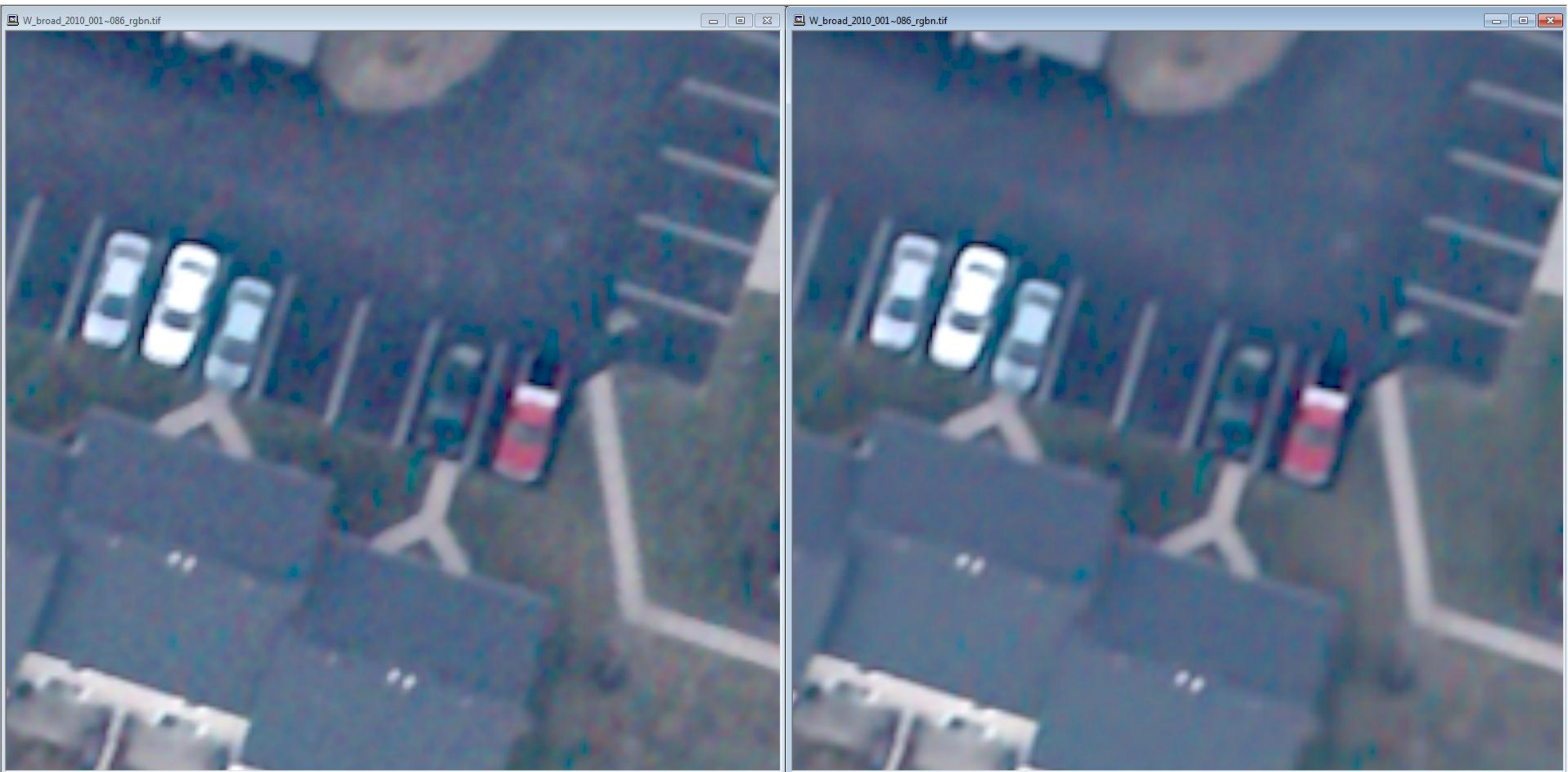

Example 2

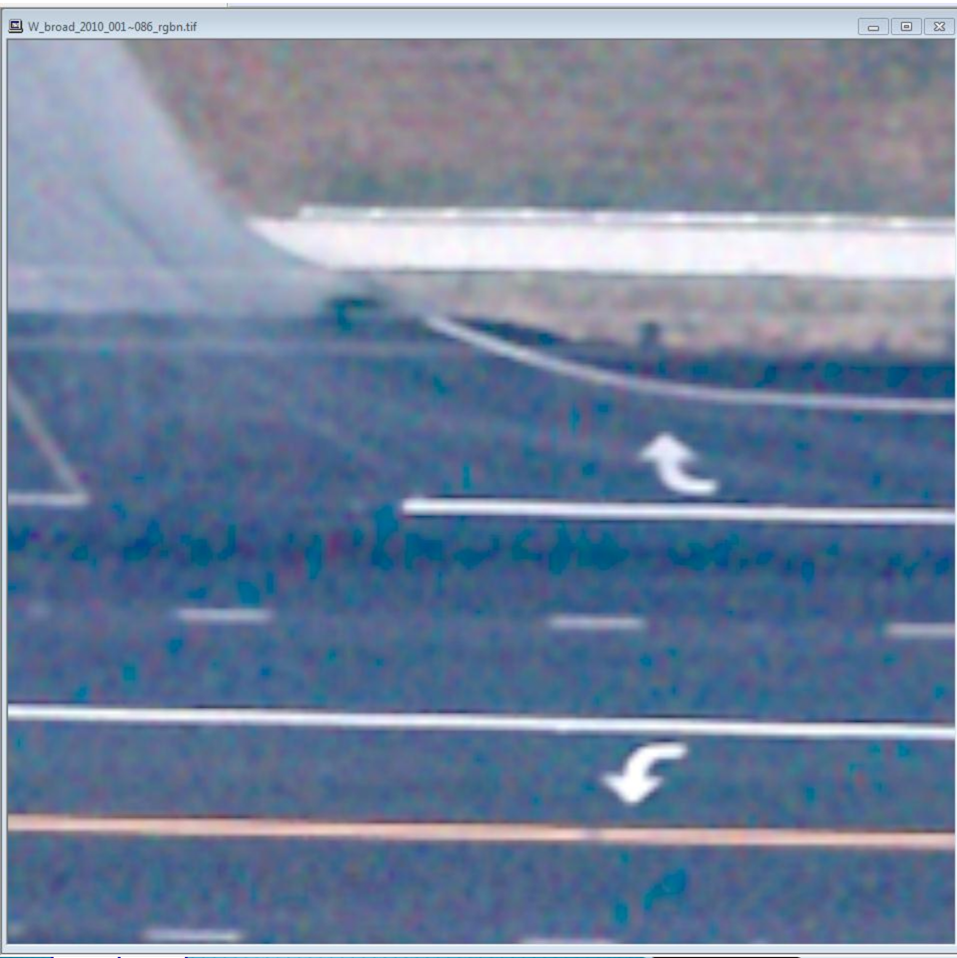

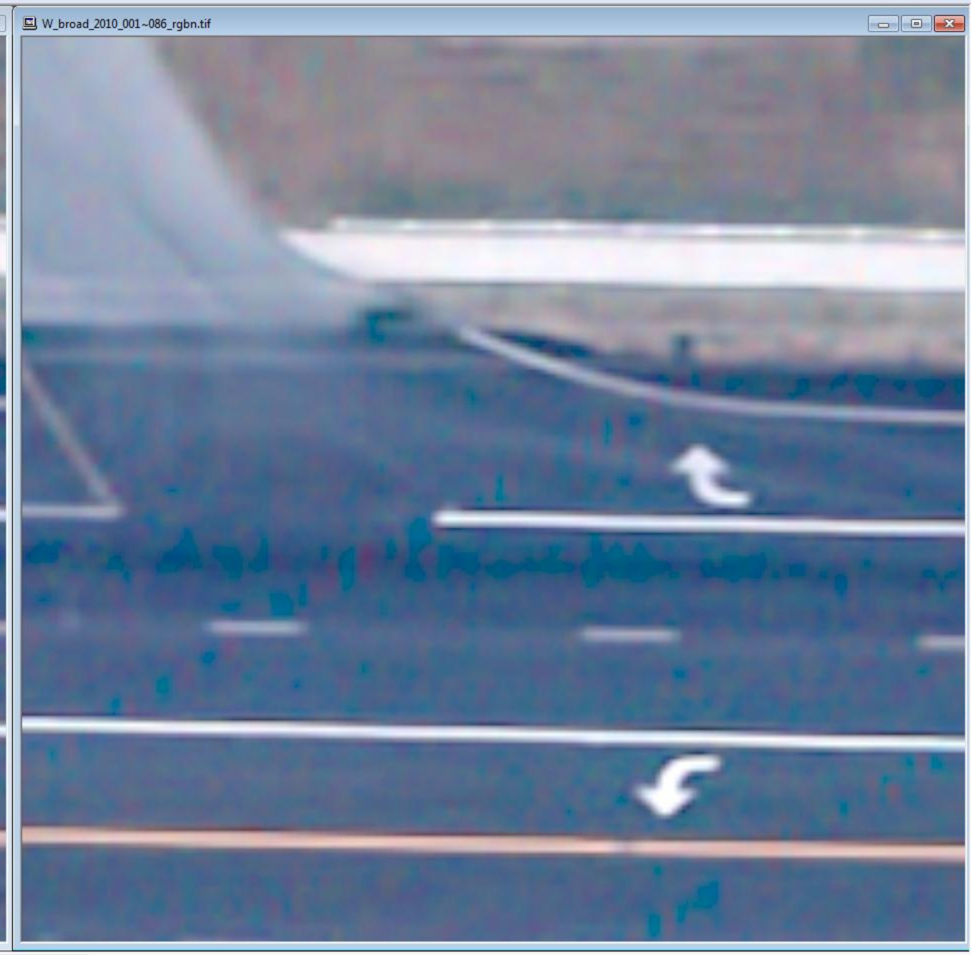

Example 3

Example 4

Example 5

Summary

- Smaller GSD and extended imaging envelopes are driving the SNR

- Denoising techniques can improve final product without significantly blurring the imagery
  - Traditional Bilateral & Sparse Methods can be used on high resolution imagery to improve SNR
  - Adaptive intra-image noise estimation techniques are needed